



1 **Blending SMAP, Noah and In Situ Soil Moisture Using Multiple Methods**

2 Ning Zhang¹, Steven M. Quiring¹, Trent W. Ford²

3

4 ¹: Department of Geography, Ohio State University;

5 ²: Illinois State Water Survey, University of Illinois at Urbana-Champaign

6 Corresponding author: Ning Zhang (zhang.7819@osu.edu)



7 **Abstract**

8 Soil moisture can be obtained from in-situ measurements, satellite observations, and model
9 simulations. This study evaluates different methods of combining model, satellite, and *in-situ* soil
10 moisture data to provide an accurate and spatially-continuous soil moisture product. Three
11 independent soil moisture datasets are used, including an *in situ*-based product that uses regression
12 kriging (RK) with precipitation, SMAP L4 soil moisture, and model-simulated soil moisture from
13 the Noah model as part of the North American Land Data Assimilation System. Triple collocation
14 (TC), relative error variance (REV), and RK were used to estimate the error variance of each parent
15 dataset, based on which the least squares weighting (LSW) was applied to blend the parent datasets.
16 These results were also compared with that using simple average (AVE). The results indicated no
17 significant differences between blended soil moisture datasets using errors estimated from TC,
18 REV or RK. Moreover, the LSW did not outperform AVE. The SMAP L4 data have a significant
19 negative bias (-18%) comparing with *in-situ* measurements, and *in-situ* measurements are valuable
20 for improving the accuracy of hybrid results. In addition, datasets using anomalies and percentiles
21 have smaller errors than using volumetric water content, mainly due to the reduced bias. Finally,
22 the *in situ*-based soil moisture and the simple-averaged product from *in situ*-based and Noah soil
23 moisture are the two optimal datasets for soil moisture mapping. The *in situ*-based product
24 performs better when the sample density is high, while the simple-averaged product performs
25 better when the station density is low, or measurement sites are less representative.

26 **Keywords:** soil moisture; in situ network; remote sensing, regression kriging; triple collocation;
27 relative error variance;

28



29 **1. Introduction**

30 Soil moisture is a critical component of the climate system. It modulates the exchange of
31 water and energy between land and atmosphere through evapotranspiration (Seneviratne et al.,
32 2010). Soil moisture has great value for understanding and predicting soil erosion and water quality
33 (Keesstra et al., 2016; Abbaspour et al., 2015), agricultural and water resource management
34 (Pittelkow et al., 2015; Dobriyal et al., 2012), runoff and flooding (Brocca et al., 2010; Wanders et
35 al., 2014), drought monitoring (Dai, 2013; Wang et al., 2011) and weather and climate forecasting
36 (Hirschi et al., 2011; Seneviratne et al., 2010). Despite the importance of soil moisture, accurate,
37 spatially-continuous soil moisture datasets with high temporal and spatial resolution are elusive.

38 There are three primary sources of soil moisture information: remote sensing (RS)
39 observations, Land Surface Models (LSMs), and in-situ measurements. Microwave remote sensing
40 is responsive to surface (~5-cm) soil moisture in regions with sparse to moderate vegetation density.
41 The passive microwave satellites that are currently in orbit include the Soil Moisture and Ocean
42 Salinity (SMOS) satellite (launched 2009, 35 km resolution, Kerr et al. (2001)), the Advanced
43 Microwave Scanning Radiometer 2 (AMSR2) (25 km resolution, Imaoka et al. (2010)) onboard
44 the GCOM-W1 satellite, and the Soil Moisture Active Passive (SMAP) satellite (launched 2015,
45 9 km resolution, Entekhabi et al. (2010)). The Advanced Scatterometer-A/B (ASCAT-A/B)
46 (Wagner et al., 2013) on board of the Meteorological Operational (METOP) satellite series
47 (launched 2006 and 2012 respectively, 25 km resolution) is an active microwave satellite in orbit.
48 The coarser spatial resolution of these sensors is compensated by their greater spatial coverage and
49 more frequent revisit times. In contrast, the active synthetic aperture radar (SAR) systems, such as
50 the one onboard the RADARSAT-2 satellite (launched 2007, 3 m resolution) (Lievens and
51 Verhoest, 2012) and the ones onboard the Sentinel-1 (A/B) satellite constellation (launched in



52 2014 and 2016, respectively, 5 m resolution) (Paloscia et al., 2013), provide soil moisture
53 information at finer spatial resolution, but with limited spatial coverage and less frequent revisit
54 times.

55 A limitation of all microwave RS soil moisture datasets is that they can only measure soil
56 moisture in the top 5 cm (or less) of the soil due to the limited penetration depth of microwave
57 signals. In addition, they cannot detect soil moisture under snow or ice, or in frozen soils. There
58 are also challenges with retrievals in areas with complex topography, dense vegetation, near water
59 bodies, or cities (Wagner et al., 1999; Parinussa et al., 2011). Ford and Quiring (2019) compared
60 the RS soil moisture datasets from SMAP (SMAP L3 and SMAP L4), SMOS and ESA-CCI with
61 in-situ measurements and found the SMAP L3 product consistently performed best among the four.

62 Model-simulated soil moisture is another source of spatially-continuous soil moisture. The
63 NOAA Climate Prediction Center (CPC) (Huang et al., 1996), Global Land Data Assimilation
64 System (GLDAS) (Rodell et al., 2004) and North American Land Data Assimilation System
65 (NLDAS) (Mitchell et al., 2004) all provide simulated soil moisture operationally at various depths
66 and time scales. Compared with in-situ measurements, Chen et al. (2013) found all four GLDAS
67 LSMs systematically underestimate the surface soil moisture in the Tibetan Plateau. Bi et al. (2016)
68 also found that all the GLDAS LSMs are strongly correlated with observations, but the Mosaic
69 model consistently has larger biases than other LSMs (the largest bias reaches $0.192 \text{ m}^3\text{m}^{-3}$) in the
70 Tibetan Plateau. By comparing GLDAS Noah model with the Standardized Precipitation Index
71 and a multi-satellite surface soil moisture product, Spennemann et al. (2015) found that GLDAS
72 Noah accurately captured the variability of soil moisture anomalies over southern South America,
73 but the accuracy varied both regionally and seasonally. Soil moisture simulations from NLDAS
74 phase 2 (NLDAS-2) are also found to have large biases when compared to in-situ observations



75 (Xia et al., 2014). Specifically, the Noah and VIC models tend to overestimate soil moisture, while
76 Mosaic and SAC models underestimate soil moisture when compared with in-situ observations
77 (Xia et al., 2015). Ford and Quiring (2019) compared the modeled soil moisture from NLDAS-2
78 and CPC with in-situ measurements and that the found NLDAS-2 models consistently performed
79 better than the CPC model.

80 Similar to RS soil moisture, model-simulated soil moisture is difficult to validate because
81 of the scale mismatch and the in-situ networks are not dense enough to adequately resolve soil
82 moisture variability within each LSM pixel. In addition, the reliability of model-simulated soil
83 moisture varies significantly from model to model, and over time and space (Ford and Quiring,
84 2019;Spennemann et al., 2015). Models generally perform well in representing the variations in
85 soil moisture and soil moisture anomalies (Downer and Ogden, 2003;Meng and Quiring,
86 2008;Albergel et al., 2012), but they tend to have large biases in simulating the absolute volumetric
87 water content of the soil (Xia et al., 2015;Bi et al., 2016).

88 In-situ soil moisture measurements from individual field campaigns and regional and
89 national soil moisture monitoring networks are invaluable for calibrating and validating LSMs and
90 RS-based soil moisture datasets and other hydrological and climatological studies. Great efforts
91 have been made to assemble, homogenize, and standardize in-situ soil moisture measurements
92 from different networks, time frames, sensors, depths and format (Cosh et al., 2016;Dorigo et al.,
93 2013;Zhang et al., 2017a;Ford and Quiring, 2014). Currently, the coordinated in-situ soil moisture
94 networks include the International Soil Moisture Network (ISMN) (Dorigo et al., 2011) and the
95 North American Soil Moisture Database (NASMD) (Quiring et al., 2016). Despite the coordinated
96 and standardized in-situ measurements, the number of stations and networks measuring soil
97 moisture continuously is still very limited at either regional or global scale. In addition, the small



98 spatial representativeness of in-situ data (a point measurement) also limits its application at larger
99 spatial scales.

100 To fully apply in-situ soil moisture on a continuous basis, a variety of approaches have
101 been adopted to generate spatial continuous soil moisture datasets based on in-situ measurements.
102 For example, Takagi and Lin (2012) used regression kriging (RK) along with five topographic
103 variables (elevation, curvature, slope, upslope contributing area, and topographic wetness index)
104 to generate soil moisture maps of the Shale Hills. The RMSE of RK predictions ranged from 0.03
105 to 0.08 m^3m^{-3} in the surface layer (0-10 cm). Yao et al. (2013) compared ordinary kriging (OK),
106 inverse distance weighting (IDW), linear regression and regression kriging (RK) to estimate soil
107 moisture at small catchment (2 km^2) with complex terrains. The auxiliary variables used in RK
108 and linear regressions were land use types, slope, and annual average solar radiation. They found
109 both OK and IDW did not perform well in complex terrains, while RK performed best with mean
110 Nash-Sutcliffe Efficiency (NSE) of 0.69 followed by linear regression. Yuan and Quiring (2017)
111 compared the reduced optimal interpolation (ROI) based on in-situ and simulated soil moisture
112 from VIC model with co-kriging and IDW methods for surface soil moisture mapping in
113 Oklahoma, and found that ROI performs better than the other two methods with a mean NSE
114 around 0.58 and a mean absolute error 0.03 m^3m^{-3} .

115 In general, the RK method performs better than other geostatistical and non-geostatistical
116 methods (Keskin and Grunwald, 2018), but it requires a relatively high density of soil moisture
117 measurements, strong correlations between soil moisture and auxiliary variables and the accurate
118 measurement of auxiliary variables (Li and Heap, 2011; Keskin and Grunwald, 2018). In addition,
119 none of the RK-gridded soil moisture datasets have been compared with the model-simulated and
120 satellite-derived soil moisture.



121 In summary, each source of soil moisture data has its strengths and weaknesses. However,
122 none of them, at least by themselves, are adequate for providing accurate soil moisture data at high
123 temporal and spatial resolutions. Therefore, it is useful to combine these three independent data
124 sources to capitalize on the strengths of each and to generate an optimal soil moisture product to
125 facilitate real-world applications. There are a number of methods that are commonly used for
126 blending together different soil moisture datasets, including triple collocation (TC) (Stoffelen,
127 1998) with least square weighting (LSW) and simple averaging (averaging parent datasets using
128 equal weighting). For example, Yilmaz et al. (2012) generated a hybrid soil moisture anomaly
129 product at 0.25° grid by merging model-derived soil moisture, thermal infrared RS-soil moisture,
130 and microwave RS-based soil moisture using TC and LSW. The TC-merged product had less
131 uncertainty, but it did not outperform the simple averaging method. Zeng et al. (2016) also used
132 TC with LSW to blend the soil moisture from two satellite (AMSRE and ASCAT) and one
133 reanalysis soil moisture product (ERA-Interim). Their merged product performed better than
134 simple averaging in the sub-humid and semi-arid regions, but the performances of TC with LSW
135 and simple averaging were similar in arid regions.

136 There are a number of knowledge gaps that still exist, including (1) of the lack of in-situ
137 soil moisture inclusion in product blending. Current studies mainly focus on combining modeled
138 and RS soil moisture, rather than combining all three sources (modeled, RS and in-situ). In-situ
139 measurements can be useful for improving the accuracy of hybrid soil moisture datasets. (2) There
140 is no comprehensive evaluation of different data blending methods. In addition to TC, there are a
141 variety of other methods that are available for combining different datasets such as Kriging and
142 Relative Error Variance (REV) (Vinnikov et al., 1996; Ford and Quiring, 2019). Therefore, it
143 would be helpful to compare the accuracy of different blending methods to identify the optimal



144 approach for soil moisture. (3) The impact of measurement units (e.g., volumetric water content,
145 soil moisture anomalies, and percentiles) is unknown. For example, is it better to convert all of the
146 soil moisture measurements to anomalies or percentiles before blending? (4) A simple and
147 operational methodology is still needed for accurate daily soil moisture mapping with high spatial
148 resolution. Current methods to generate gridded soil moisture data products cannot produce data
149 with sufficient spatial resolution for many agricultural and hydrological applications.

150 This paper addresses all four of these knowledge gaps by assessing different blending
151 methods to merge model-simulated, RS-based and in-situ soil moisture data into a 4-km soil
152 moisture product. The impact of different measurement units (absolute, anomalies and percentiles)
153 on the accuracy of the blended product are also investigated. Finally, two optimal datasets are
154 identified and the utility of these datasets are demonstrated.

155 **2. Study area and data**

156 This study is conducted in the south-central region of the United States, covering four states,
157 including Texas, Oklahoma, Arkansas, and Louisiana with a total area $\sim 1,150,400 \text{ km}^2$. The south-
158 central U.S. an important agricultural region in the U.S., but also one that is drought-prone (Tian
159 and Quiring, 2019). For example, the four states account for about 10% of national winter wheat
160 production in 2017 (National Agricultural Statistics Service). According to the Köppen climate
161 classification, the climate of this region varies from warm temperate (about three-fourths of the
162 region) in the east to the arid (about one-fourth of the region) in the west (Kottek et al., 2006). The
163 annual average temperature gradually decreases from south ($27 \text{ }^\circ\text{C}$) to north ($13 \text{ }^\circ\text{C}$), and the mean
164 annual precipitation gradually increases from west ($<25 \text{ cm}$) to east ($>190 \text{ cm}$).

165 This study uses in-situ measurements of soil moisture, satellite-observed soil moisture,
166 model-simulated soil moisture, precipitation and air temperature data. Detailed information on the



167 spatial and temporal resolution, period of record and measurement depths are listed in Table 1. To
 168 facilitate comparison, the common period of record from 2015/03/31 to 2018/12/31 (SMAP
 169 product) were extracted for all datasets.

170

171 Table 1. Summary of datasets used in this study

Data Sources		Temporal Domain	Temporal resolution	Spatial resolution*	Measurement depths (cm)
In-situ	OKM	1998-present	Daily	115 out of 129 sites	5, 25, 60, 75
	WTM	2002-present	Daily	64 out of 70 sites	5, 20, 60, 75
	SCAN	1994-present	Daily	21 out of 219 sites	5, 10, 20, 50, 100
	CRN	2009-present	Daily	15 out of 147 sites	5, 10, 20, 50, 100
SMAP L4		2015/03/31 - present	3 hours; latency: 2 days	9-km	5, 0-100
NLDAS_V2 Noah Model		1979-present	Hourly	1/8°	0-10, 10-40, 40-100
PRISM	ppt, tmp	1981-present	Daily	4-km	

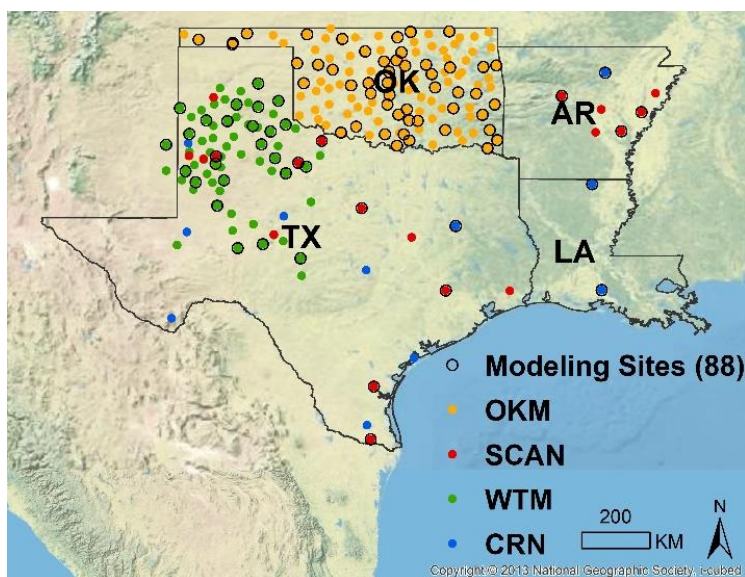
172 *: The in-situ measurements are point-based, thus the spatial resolution for in-situ data refers to
 173 the number of stations used in this study out of a total number of stations of the sparse network.
 174

175 2.1 In-Situ Soil Moisture Measurements

176 The in-situ soil moisture data are collected from four sparse networks: Oklahoma Mesonet
 177 (OKM), West Texas Mesonet (WTM), Soil Climate Analysis Network (SCAN) and Climate
 178 Reference Network (CRN). Daily soil moisture measurements were obtained from North
 179 American Soil Moisture Database (NASMD) in the units of volumetric water content ($m^3 m^{-3}$)
 180 (Quiring et al., 2016). Since different networks collect data at different time intervals ranging from
 181 every 5 minutes to once per day, for consistency a single morning measurement (7 am LST) is
 182 extracted to represent the daily value. This is not ideal, but it is reasonable for applications in which
 183 diurnal variations in soil water content are inconsequential, such as drought monitoring. The raw



184 measurements have passed through the Quality Assurance and Quality Control (QAQC) process
185 (Ford and Quiring, 2014), with dubious or questionable values been removed and filled. The near-
186 surface measurements (5 cm) from a total of 215 stations (Fig. 1) were obtained for this study.



187
188 **Fig. 1** Study area and stations for in-situ soil moisture measurements. Background map (USA
189 Topographic Basemap) Copyright:© 2013 National Geographic Society, i-cubed

190 2.2 SMAP-L4 Soil Moisture

191 The SMAP Level-4 Surface and Root-Zone Soil Moisture are adopted in this study because
192 it provides a temporally complete set of global soil moisture data. The SMAP L4 product is a
193 merged soil moisture product from SMAP L-band brightness temperature observations and
194 estimates from the NASA Catchment land surface model using a data assimilation system (Reichle
195 et al., 2018). The L4 Geophysical Data are used, which are available from 31 March, 2015 to
196 present (with 2-3 days latency). They include both surface (0-5 cm) and root-zone (0-100 cm) soil
197 moisture every 3 hours at a spatial resolution of 9-km. The unbiased RMSE for SMAP L4_SM
198 surface and root zone soil moisture are reported to be $0.038 \text{ m}^3 \text{ m}^{-3}$ and $0.030 \text{ m}^3 \text{ m}^{-3}$ respectively



199 (Reichle et al., 2017). Finally, to be consistent with the in-situ measurements, the SMAP L4
200 product with time slot covering 7 am are extracted each day to represent the daily soil moisture
201 from 2015/03/31 to 2018/12/31. The nearest neighbor assignment is used to resample SMAP L4
202 surface soil moisture from 9-km to 4-km to match the spatial resolution of other datasets (e.g.,
203 PRISM).

204 **2.3 NLDAS-2 Noah Soil Moisture**

205 This study uses the simulated soil moisture from the NLDAS-2 Noah model. The Noah
206 model provides hourly soil moisture fields at $1/8^\circ$ grid from 1979 to present. The Noah model has
207 four soil layers: 0–10 cm, 10–40 cm, 40–100 cm, and 100–200 cm, but only the top layer is used
208 in this study. Details about the NLDAS-2 configuration of the Noah LSM can be found in Xia et
209 al. (2012). To be consistent with the in-situ measurements, the Noah output at 7 am are extracted
210 each day to represent the daily soil moisture, and the data from 2015 to 2018 are adopted to match
211 the record length of the SMAP data. Finally, the nearest neighbor method is used to resample the
212 simulated soil moisture from 12.5-km to 4-km to match with other datasets.

213 **2.4 PRISM Climate Data**

214 The PRISM (Parameter-elevation Relationships on Independent Slopes Model) datasets
215 are developed by Oregon State University's PRISM Climate Group (Daly et al., 2008). They are
216 official climatological data sets of the USDA. PRISM use surface stations and a weighted
217 regression scheme to generate daily updated spatial mapping of climate variables (e.g.,
218 precipitation, temperature, dew point, vapor pressure deficit) over the contiguous United States.
219 There are more than 13,000 quality controlled surface stations used for precipitation interpolation
220 and more than 10,000 stations used for temperature interpolation (Daly et al., 2008). The



221 climatological normals (average monthly and annual conditions over 1981-2010) and monthly and
222 daily data are available at 4-km and 800-m resolution from 1981 to present.

223 The 4-km daily precipitation from PRISM are used in this study. Since there is strong
224 coupling between soil moisture and precipitation (Koster et al., 2004), precipitation has been
225 widely used as an important input for soil moisture estimation in various LSMs (Liu et al.,
226 2018; Xia et al., 2012; Liang et al., 1996). Here, the Antecedent Precipitation Index (API) is
227 calculated based on precipitation and adopted for soil moisture interpolation using in-situ
228 measurements and regression kriging. The API index is introduced in Section 2.5.2 and regression
229 kriging is introduced in Section 3.

230 **2.5 Data Preparation**

231 2.5.1 Anomalies and Percentiles

232 The volumetric water content of the soil varies as a function of weather conditions, soil
233 characteristics, vegetation, topography, among other factors, and so it cannot be directly compared
234 between different locations. In contrast, relative measures of soil wetness, such as anomalies and
235 percentiles can be used to standardize soil moisture from different sensors and locations and make
236 them comparable (Ford et al., 2015; Zhang et al., 2017a). In this study, anomalies and percentiles
237 are calculated for all 3 datasets (In-situ, SMAP, NLDAS and PRISM). Anomalies are calculated
238 by removing the seasonal climatology from the absolute soil moisture at each day (Crow and Van
239 den Berg, 2010). The climatological mean is calculated using a moving-window approach (Chen
240 et al., 2017), which averages all available soil moisture estimates across all years within a 31-day
241 window (Dong et al., 2018) centered on the target day.

242 Percentiles are calculated using an empirical probability distribution function and moving
243 window approach as well. At each day of the year, all the data fall within a 31-day window centered



244 on that day was used to construct the empirical probability distribution function. Ford et al. (2016)
245 found sample sizes of 93 to 186 daily soil moisture observations were required to generate robust
246 percentiles. In our case, SMAP has the shortest data record (3 years), thus has 93 data points (31
247 days in window \times 3 years) from which to build the distribution and compute the quartiles and
248 percentiles. This has met the sampling size to generate robust percentiles. For other datasets, the
249 total length of records is used to generate the percentiles (e.g., 20 years for in-situ, 40 years for
250 NLDAS). Percentiles range from 0 or (0%) to 1 (or 100%), which corresponds to the driest (0%)
251 and wettest (100%) soil conditions at a specific site over the entire study period.

252 2.5.2 Antecedent Precipitation Index (API)

253 The API is precipitation-based moisture index. It is used to indicate the wetness of a
254 location and has been widely applied in drought monitoring (Crow et al., 2012a), runoff forecasting
255 (Anctil et al., 2004), soil moisture estimation (Ochsner et al., 2019) and crop yield prediction
256 (Zhang et al., 2017b). API takes preceding precipitation into account to estimate the current
257 moisture status, and is formulated as (Kohler and Linsley, 1951):

$$258 \quad \text{API}(i) = \text{API}(i - 1) * k + \text{PPT}(i) \quad (1)$$

259 Where $\text{API}(i)$ is the API at day i , $\text{PPT}(i)$ is the precipitation occurring on day i ; k is an
260 empirical decay factor between 0.80 and 0.98 (Heggen, 2001). In this study, a set of k values (from
261 0.80 to 0.99) is tested to determine the optimal k value that results in the highest correlation
262 between API and soil moisture based on 215 stations. Fig. S1 shows the variation in correlation as
263 a function of different k values. The highest correlation ($r = 0.4$) is achieved at $k = 0.92$. Therefore,
264 $k = 0.92$ is used in this study for API calculation.



265 2.5.3 Site Selection

266 In this study, 40% of the stations with soil moisture measurements (88 sites) are used for
267 modeling (black circles in Fig. 1), while the remaining 60% of stations (127 sites) are used for out-
268 of-sample validation. The 88 modeling sites are selected based on the Index of Temporal Stability
269 (ITS) (Jacobs et al., 2010; Zhao et al., 2010). ITS is an indicator of the temporal representative
270 locations. The location with the lowest ITS value is the location with the highest temporal stability.
271 The ITS at location i (ITS_i) is calculated as:

$$272 \quad ITS_i = \sqrt{MRD_i^2 + SDRD_i^2} \quad (2)$$

$$273 \quad MRD_i = \frac{1}{T} \sum_{j=1}^T RD_{i,j} \quad (3)$$

$$274 \quad SDRD_i = \sqrt{\frac{1}{T-1} \sum_{j=1}^T (RD_{i,j} - MRD_i)^2} \quad (4)$$

$$275 \quad RD_{i,j} = \frac{\theta_{ij} - \bar{\theta}_j}{\bar{\theta}_j} \quad (5)$$

276 Where θ_{ij} is individual daily measurement of soil moisture at location $i \in [1, \dots, N]$ and
277 time $j \in [1, \dots, T]$, and $\bar{\theta}_j$ is the spatial average of soil moisture at all locations at time j . $RD_{i,j}$ is
278 the relative difference of location i at time j , which is introduced by Vachaud et al. (1985). MRD_i
279 is the mean relative difference of location i . It averages the RD at location i across an entire period
280 (T days), and represents the location's temporal bias or whether the location is wetter or drier than
281 the average of the area during T days. $SDRD_i$ is the standard deviation of the RD at location i . It
282 describes the degree of the temporal stability of a location, or whether a location is temporally
283 stable. Therefore, a temporally representative site is one with a small mean bias and can be
284 characterized by low values of both MSD and SDRD, and a low value of ITS (Cho and Choi,
285 2014; Penna et al., 2013; Brocca et al., 2012).



286 Since anomalies can be negative, the absolute value of the difference between $A_{i,j}$ and \bar{A}_j
287 (Eq. 6) is adopted to represent the relative difference of anomalies at location i and time j ($RD_{A_{ij}}$)
288 (Wang et al., 2017;Mittelbach and Seneviratne, 2012):

$$289 \quad RD_{A_{ij}} = |A_{i,j} - \bar{A}_j| \quad (6)$$

290 where $\bar{A}_j = \frac{1}{N} \sum_{i=1}^N A_{ij}$, indicates the spatial average of anomalies of all stations at time j .

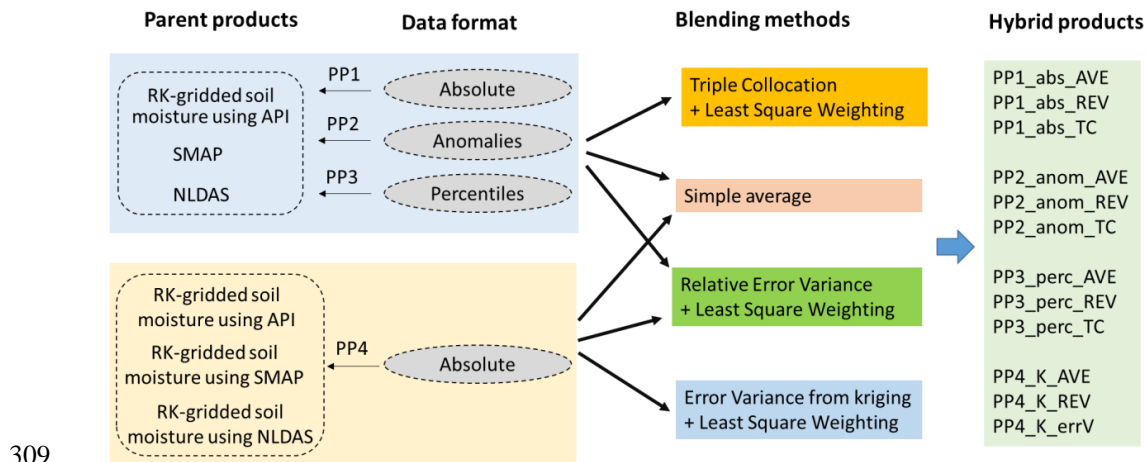
291 In this study, the 88 modeling sites are selected by three steps: (1) Calculate and rank the
292 ITS of 215 stations in ascending order; (2) Evenly divide the ranked ITS into four groups; (3)
293 Within each group, select the 22 sites with the smallest ITS values. The 88 sites are selected in this
294 way to ensure an evenly sampled sites across the ITS range, which best mimic the reality that in-
295 situ stations have different temporal representativeness. Although ITS ranking using absolute soil
296 moisture, anomalies and percentiles are not exactly the same, the differences are minor. To be
297 consistent across datasets and facilitate comparison, the same 88 (127) sites selected using the
298 absolute soil moisture were used for calibration (validation) using soil moisture anomalies and
299 percentiles, because the selected sites are also evenly distributed within the ITS range calculated
300 by anomalies and percentiles (Fig. S2).

301 **3. Blending Methods**

302 The soil moisture blending schemes used in this study are summarized in Fig. 2. Two
303 categories of parent datasets are adopted in this study (Fig. 2). The first category is consist of
304 SMAP observations, NLDAS simulations, and RK-gridded soil moisture using in-situ soil
305 moisture and API. The datasets from the first category are implemented with three data formats:
306 absolute values (PP1), anomalies (PP2), and percentiles (PP3). The second category consists of



307 the RK-gridded soil moisture (PP4) using in-situ soil moisture with the absolute values of API,
 308 SMAP, and NLDAS soil moisture respectively.



309
 310 **Fig. 2** Framework of soil moisture blending, and their associated parent datasets, data format,
 311 blending methods and output products.

312 3.1 Regression Kriging (RK)

313 Regression Kriging (RK) is one of the most popular and robust hybrid spatial interpolation
 314 techniques in the digital mapping of soil properties (Keskin and Grunwald, 2018). RK combines a
 315 regression between the target variable and auxiliary variables with simple kriging of the regression
 316 residuals (Hengl et al., 2007; Odeh et al., 1994). Previous studies revealed RK often outperforms
 317 non-geostatistical methods (Mishra et al., 2010; Yang et al., 2019; Li and Heap, 2011), ordinary
 318 kriging (Hengl et al., 2004), and co-kriging (Eldeiry and Garcia, 2010). The RK models can be
 319 expressed as two parts (Hengl et al., 2004):

$$320 \hat{z}(s_0) = \hat{m}(s_0) + \hat{e}(s_0) \quad (7)$$

321 Where $\hat{m}(s_0)$ is the fitted trend, $\hat{e}(s_0)$ is the interpolated residual. In this study, the trend term
 322 $\hat{m}(s_0)$ is fitted by a linear model between the auxiliary variable and soil moisture.

$$323 \hat{m}(s_0) = \hat{\beta} \cdot q(s_0) \quad (8)$$



324 Where, $\hat{\beta}$ is the estimated model coefficients using generalized least squares, $q(s_0)$ is the auxiliary
325 variable (e.g., API) at the target location s_0 . The residual from the linear model is then interpolated
326 by simple kriging with an assumed 0 mean.

$$327 \quad \hat{e}(s_0) = \sum_{i=1}^n \lambda_i \cdot e(s_i) \quad (9)$$

328 Where, λ_i are kriging weights determined by the spatial dependence structure of the residual, and
329 $e(s_i)$ is the residual at location s_i . By adding the kriging residuals to the predicted trend, the final
330 RK prediction are obtained. RK also provide the error estimation of predicted values as (Hengl et
331 al., 2007):

$$332 \quad \sigma_{RK}^2(s_0) = (C_0 + C_0) - c_0^T \cdot C^{-1} \cdot c_0 + (q_0 - q^T \cdot C^{-1} \cdot c_0)^T \cdot (q^T \cdot C^{-1} \cdot q)^{-1} \cdot (q_0 - q^T \cdot C^{-1} \cdot$$

333 $c_0)$ (10)

334 Where C is the covariance matrix of the residuals, $C_0 + C_0$ is the sill variation, c_0 is the vector of
335 covariance of residuals at the unvisited locations, q is a matrix of predictors at the sampling
336 locations, and q_0 is the vector of $p+1$ predictors ($p=1$ in our case).

337 In this study, two sets of auxiliary variables are tested for RK. The first set of auxiliary
338 variables are API in the format of absolute values, anomalies, and percentiles respectively. Given
339 that precipitation is the chief driver of soil moisture, and a strong positive relationship was
340 observed between the soil moisture and API over the contiguous United States (Fig. S3), thus API
341 can be used as an important predictor of soil moisture variations. The second set of auxiliary
342 variables are respectively the SMAP L4 and the NLDAS surface soil moisture in the format of
343 volumetric water content (Fig. 2).

344 **3.2 Triple collocation (TC)**

345 Triple collocation (TC) is a technique for estimating the error variance (errVar , $\text{m}^3 \text{m}^{-3}$) of
346 three independent datasets with respect to the unknown truth (Stoffelen, 1998). It assumes a linear



347 error model (Eq. 11- Eq.13) between each product and the unknown truth (t). The errors from the
348 independent sources are assumed to have zero mean ($E(e_i) = 0$) and are uncorrelated with each
349 other ($Cov(e_i, e_j) = 0, i \neq j$) and with the truth ($Cov(e_i, t) = 0$). TC analysis has been widely
350 used to estimate the errors of various measurement systems, such as the ocean waves (Caires and
351 Sterl, 2003), wind fields (McColl et al., 2014;Stoffelen, 1998), leaf area index (Fang et al., 2012),
352 precipitation (Roebeling et al., 2012), and soil moisture (Su et al., 2014;Yilmaz et al., 2012;Dorigo
353 et al., 2010;Gruber et al., 2013). Gruber et al. (2016) reviewed the previous TC analysis on soil
354 moisture, and found there are two different notations of TC formula, the difference notation
355 (Stoffelen, 1998;Scipal et al., 2008;Yilmaz et al., 2012) and the covariance notation (Stoffelen,
356 1998;McColl et al., 2014). They demonstrated that two different notations are mathematically
357 identical in the ideal case that each product is bias-free ($\alpha_i = 0$ in Eq. 11 to Eq. 13). However, in
358 reality, there is always bias in each product, which results in a slightly different value of errVar
359 estimated using the two notations. The difference notation format of TC accounts for the total
360 errVar (including variance from both bias α_i and error term e_i), while the covariance notation of
361 TC only focuses on the errVar from the error term (e_i). In this study, the difference notation of TC
362 is adopted to account for the total error variance of parent datasets.

$$363 \quad \theta_K = \alpha_K + \beta_K \theta_t + e_K \quad (11)$$

$$364 \quad \theta_S = \alpha_S + \beta_S \theta_t + e_S \quad (12)$$

$$365 \quad \theta_N = \alpha_N + \beta_N \theta_t + e_N \quad (13)$$

366 Where, θ_i ($i \in (S, N, K)$) are three collocated soil moisture datasets for SMAP, NLDAS
367 and RK-gridded soil moisture, respectively; θ_t is the unknown true soil moisture; α_i ($i \in (K, S,$
368 $N)$) and β_i ($i \in (K, S, N)$) are systematic additive and multiplicative biases of product i with respect
369 to the truth, and e_i ($i \in (K, S, N)$) are the additive zero-mean random errors for each system. When



370 anomalies or percentiles are used, the additive bias α_i can be deemed as zero, because these two
371 methods either removed the climatology mean from each product or standardized each product.

372 A reference dataset must be selected from the three input datasets and rescaling is required
373 to transfer the other two datasets into the same observation space of the reference dataset. Our
374 preliminary results showed that the choice of reference dataset did not impact the final results, thus
375 the RK-gridded soil moisture is selected as the reference dataset in this study ($\theta_R = \theta_K$). The
376 rescaling method (Eq. 14) from Dorigo et al. (2010) is used.

$$377 \quad \theta_i^* = \bar{\theta}_R + \sqrt{\frac{VAR(\theta_R)}{VAR(\theta_i)}} \cdot (\theta_i - \bar{\theta}_i) \quad (14)$$

378 Where, $\bar{\theta}_R$ and $VAR(\theta_R)$ are respectively the mean and variance of the reference soil moisture.
379 After the rescaling of the parent datasets, Eq. (11) to (13) can be rewritten as:

$$380 \quad \theta_K^* = \beta_K \theta_t + e_K^* \quad (15)$$

$$381 \quad \theta_S^* = \beta_S \theta_t + e_S^* \quad (16)$$

$$382 \quad \theta_N^* = \beta_N \theta_t + e_N^* \quad (17)$$

383 where, θ_i^* ($i \in (K, S, N)$) are the rescaled soil moisture datasets. Finally, the error variances can be
384 estimated by averaging the cross-multiplied differences between the three datasets:

$$385 \quad \sigma_K^{*2} = \overline{(\theta_K^* - \theta_S^*)(\theta_K^* - \theta_N^*)} \quad (18)$$

$$386 \quad \sigma_S^{*2} = \overline{(\theta_S^* - \theta_K^*)(\theta_S^* - \theta_N^*)} \quad (19)$$

$$387 \quad \sigma_N^{*2} = \overline{(\theta_N^* - \theta_S^*)(\theta_N^* - \theta_K^*)} \quad (20)$$

388 Different combinations of triplets are also tested in this study to examine the impact of
389 triplets on TC estimates. The triplet candidates include the in-situ measurements (denoted by “I”
390 in the following figure and text), the SMAP L-4 surface soil moisture (denoted by “S”), simulated
391 soil moisture from NLDAS-2 Noah model (denoted by “N”), and the RK-gridded soil moisture



392 using regression kriging (denoted by “K”). Four combinations of the candidates are tested,
393 including (I, S, N), (I, K, S), (I, K, N), and (K, S, N). The triplet candidates are extracted from the
394 127 out-of-sample stations. Scipal et al. (2008) found at least 100 collocated triplet samples are
395 required for a reliable estimation of the variance. In our case, the time series from 2015/03/31 to
396 2018/12/31 is used for TC analysis, which results in 1372 collocated triplet samples at every station
397 with a serially complete record. The stations with less than 100 observations are removed from the
398 TC error estimation.

399 **3.3 Relative Error Variance (REV)**

400 Relative Error Variance (REV) is the ratio of measurement error variance to real soil
401 moisture variance. It measures the displacement of autocorrelation in a measured quantity.
402 Delworth and Manabe (1988) recognized that a soil moisture time series behaves like a first-order
403 Markov process. Later Vinnikov and Yeserkepova (1991) validated and confirmed this and noted
404 the autocorrelation function of soil moisture can be expressed as an exponential form of lag length:

$$405 \quad \gamma(\tau) = \exp(-\tau/T) \quad (21)$$

406 where $\gamma(\tau)$ is the autocorrelation function, τ is the lag, and T is the decay time scale. Robock et
407 al. (1995) also found a linear best fit of $\ln(\gamma)$ verse τ does not cross zero at a value of $\gamma(\tau = 0) =$
408 1. The displacement of the autocorrelation $\gamma(\tau)$ at $\tau = 0$ is related to the measurement error (a) as:

$$409 \quad \gamma(\tau = 0) = 1 - a \quad (22)$$

410 Successively, Vinnikov et al. (1996) partitioned the soil moisture variation into red noise
411 (σ^2 , actual variance of the soil moisture measurement) and white noise (δ^2 , random error of
412 measurements), and noted that the ratio δ^2/σ^2 can be used as a measure of the random error in the
413 measurement. Dirmeyer et al. (2016) related the ratio δ^2/σ^2 to the measurement error (a), and
414 used it to estimate the random measurement error of different sparse soil moisture networks. Ford



415 and Quiring (2019) applied relative error variance (REV) to quantify the proportion of
416 measurement error within real soil moisture variance, as:

$$417 \quad REV = \frac{\delta^2}{\sigma^2} = \frac{a}{(1+a)} \quad (23)$$

418 Thus, a higher REV value represents a larger proportion of random measurement error.
419 REV is a powerful measurement of random measurement error or uncertainties, and it does not
420 require independent data, unlike the TC method.

421 **3.4 Least square weighting (LSW)**

422 Yilmaz et al. (2012) adopted the least square framework to achieve an objective blending
423 of satellite and modeled soil moisture. The same methodology was adopted by Zeng et al. (2016)
424 to merge the satellite and reanalysis soil moisture data. In this study, the least square weighting
425 (LSW) is used to blend soil moisture data from satellite, model and in-situ measurements based on
426 error variances estimated from the TC, REV and RK methods, respectively (Fig. 2). The desired
427 estimate of soil moisture (S_m) via blending different sources of data using least squares framework,
428 can be expressed as:

$$429 \quad S_m = w_x S_x + w_y S_y + w_z S_z \quad (24)$$

430 Where, w_x , w_y and w_z are the relative weights of three parent datasets S_x , S_y and S_z respectively.
431 Then a cost function (J) is constructed using the weights and the error variance of the parent
432 datasets, such that:

$$433 \quad J = \sigma_m^2 = w_x^2 \sigma_x^2 + w_y^2 \sigma_y^2 + w_z^2 \sigma_z^2 \quad (25)$$

434 Where, σ_x^2 , σ_y^2 , and σ_z^2 are the estimated error variance for the three parent datasets. To have an
435 unbiased estimation of S_m , the sum of weights should be 1 ($w_x + w_y + w_z = 1$), thus:

$$436 \quad J = w_x^2 \sigma_x^2 + w_y^2 \sigma_y^2 + (1 - w_x - w_y)^2 \sigma_z^2 \quad (26)$$



437 Finally, by minimizing the cost function and the partial derivative of function J with respect
438 to w_x and w_y ($\frac{\partial J}{\partial w_x} = 0, \frac{\partial J}{\partial w_y} = 0$), the optimal estimation of the weights are obtained as

$$439 \quad w_x = \frac{\sigma_y^2 \sigma_z^2}{\sigma_x^2 \sigma_y^2 + \sigma_x^2 \sigma_z^2 + \sigma_y^2 \sigma_z^2} \quad (27)$$

$$440 \quad w_y = \frac{\sigma_x^2 \sigma_z^2}{\sigma_x^2 \sigma_y^2 + \sigma_x^2 \sigma_z^2 + \sigma_y^2 \sigma_z^2} \quad (28)$$

$$441 \quad w_z = \frac{\sigma_x^2 \sigma_y^2}{\sigma_x^2 \sigma_y^2 + \sigma_x^2 \sigma_z^2 + \sigma_y^2 \sigma_z^2} \quad (29)$$

442 It can be seen that the weights are functions of the error variance of the parent datasets, and
443 the product with larger error variance will be given smaller weights and vice versa. If only blending
444 two soil moisture datasets, the least square method can be applied similar, with weights:

$$445 \quad w_x = \frac{\sigma_y^2}{\sigma_x^2 + \sigma_y^2} \quad (30)$$

$$446 \quad w_y = \frac{\sigma_x^2}{\sigma_x^2 + \sigma_y^2} \quad (31)$$

447 In this study, all three parent datasets (K, S, N) and combinations of two from them (KS,
448 KN, SN) are tested to generate hybrid datasets. By comparing the hybrid results using all three and
449 two out of three datasets, the optimal blending product can be identified using the least datasets
450 while maintaining the accuracy.

451 **3.5 Goodness of fit**

452 In this study, 88 sites (40%) out of the total 215 stations were used for RK modeling, while
453 the remaining 127 sites (60%) were used for out-of-sample validation. The Mean Absolute Error
454 (MAE), Root Mean Square Error (RMSE), the Nash-Sutcliffe Efficiency (NSE) score, and the
455 decomposition of Mean Square Error (MSE) by its mean difference (MSE_MD²) and its pattern
456 variation (MSE_VAR) were used for the validation and comparison of hybrid datasets. The



457 decomposition MSE is helpful to diagnose whether the error is mainly due to the bias or variation.
458 A detailed description of above mentioned indicators (including equations) are provided in
459 Supplementary Text S1.

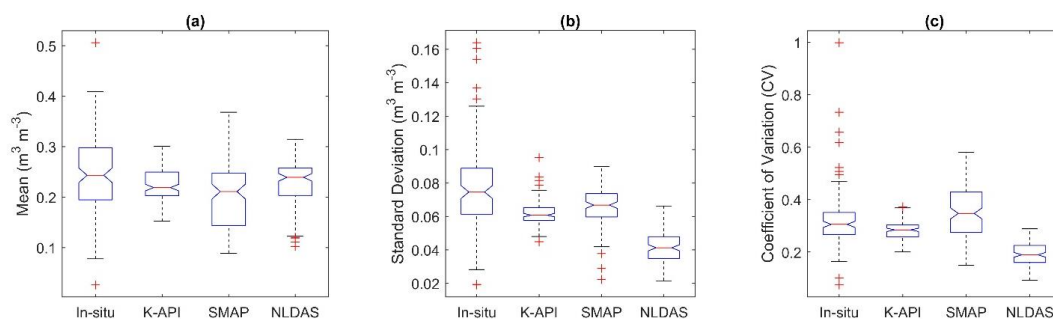
460 **4. Results and Discussions**

461 **4.1 Patterns of parent datasets**

462 Fig. 3 compares three statistic features, such as mean, standard deviation (STD) and
463 coefficient of variation (CV) of the absolute values of four soil moisture datasets over 127 out-of-
464 sample sites. The four datasets include the in-situ soil moisture measurements, the RK-gridded soil
465 moisture from API (K-API) and the SMAP and NLDAS soil moisture. Compared with in-situ
466 measurements, the three soil moisture datasets (K-API, SMAP and NLDAS) show an
467 underestimation of soil moisture (Fig. 3a) with bias ratios of -9%, -18% and -8%, respectively.
468 The large negative bias of SMAP L4 data indicates that the produce may overestimate dryness if
469 used alone without animalization or standardization. The largest values of STD are observed for
470 in-situ soil moisture, followed by SMAP and K-API, while NLDAS has the smallest STD values
471 (Fig. 3b). This is reasonable since field measurements are point scale and contain more information
472 on spatial heterogeneity and thus exhibit a higher degree of variability. As spatial resolution
473 increases, a smoother pattern and less variability are expected. Another reason that NLDAS has
474 the smallest STD is because the model-simulated soil moisture are solved at each grid cell using a
475 land surface model. SMAP presents the highest (and significantly larger than others) CV among
476 all datasets (Fig. 3c), which indicates that there is a large degree of variability in the SMAP soil
477 moisture. The large CV of SMAP is jointly attributed to its small mean value and large STD. In
478 contrast, the NLDAS has the smallest CV among all datasets (Fig. 3c), which is mainly due to its
479 smallest STD among all datasets. K-API has the most comparable CV values and smaller range



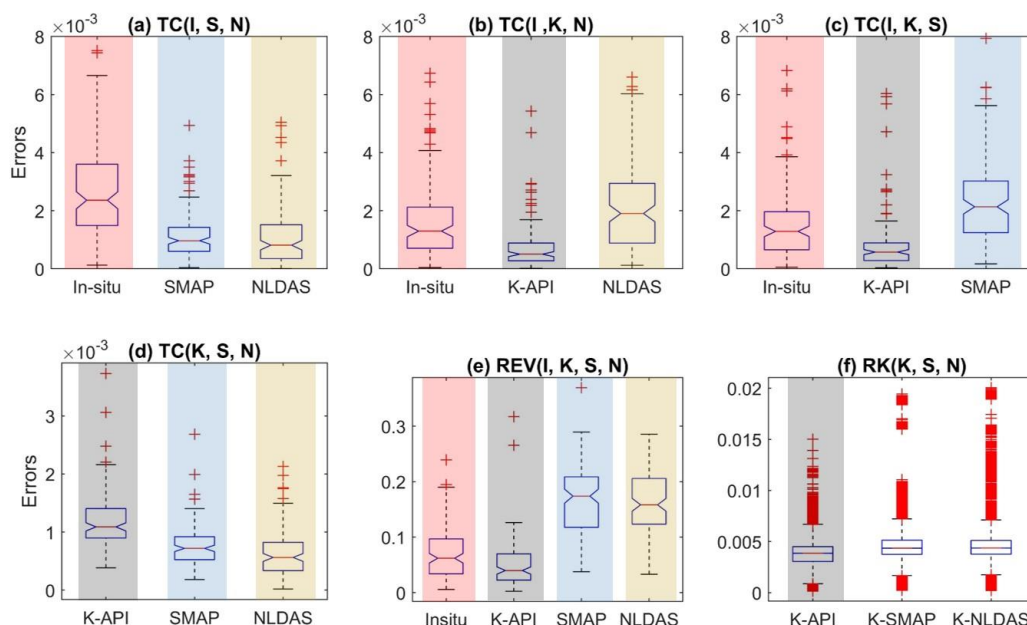
480 than that of in-situ measurements. This indicates that K-API is the product that is most similar to
481 the in-situ measurements.



482
483 **Fig. 3** Comparison of the (a) means, (b) standard deviation and (c) coefficient of variation of four
484 datasets over 127 out-of-sample sites. The four data sets include the in-situ soil moisture
485 measurements, the kriged soil moisture from API (K-API) and the SMAP and NLDAS soil
486 moisture. All datasets are in the format of absolute values.

487 4.2 Errors of parent datasets

488 Fig. 4 shows the error (uncertainties) estimated using TC, REV and RK using different
489 combinations of parent datasets. Fig. 4 (a)-(d) reveal that the error estimated from TC depends on
490 the parent triplets used. Changing the parent triplets changes the magnitude and ranking of the
491 parent datasets. For example, the errors estimated for in-situ data are higher when it is grouped
492 with SMAP and NLDAS (Fig. 4a), than when it is grouped with K-API and NLDAS (Fig. 4b) or
493 with K-API and SMAP (Fig. 4c). In addition, in-situ data have significantly higher errors than
494 SMAP in Fig. 4(a), while Fig. 4c shows in-situ data have significantly lower errors than that of
495 SMAP. Similar, contrasting results are also found between In-situ and NLDAS by comparing Fig.
496 4a and Fig. 4b. These results indicate that TC only provides a relative measure of accuracy. Yilmaz
497 et al. (2012) also noted that TC is not ideal for capturing absolute error and can only estimate the
498 relative error. They found that the absolute error depends on the reference dataset selected.



499

500 **Fig. 4** (a)-(d) Estimated errors (uncertainties) using TC with different combination of four datasets
501 (In-situ, K-API, SMAP and NLDAS soil moisture). (e) Estimated errors using REV for four
502 datasets; and (f) Estimated errors using RK for three datasets (K-API, SMAP and NLDAS soil
503 moisture). The datasets used here are absolute soil moisture over 127 out-of-sample stations. The
504 same color indicates the same dataset used in TC and REV analysis. Note, both TC and REV
505 provide one error estimation through the entire period (1372 days) for each station, while RK
506 provides one error estimation at each day for each station. Therefore, there are 127 points within
507 the boxplots using TC and REV (Fig. 6a-e), while there are 174244 points (127 sites*1372 days)
508 within the boxplots using RK (Fig. 6f).

509 Moreover, our study reveals that the relative errors of a single soil moisture dataset,
510 estimated from TC, are sensitive to the choice of input datasets (Fig. 4a-d). Thus, caution should
511 be used when selecting the input datasets for TC analysis. In this study, K-API, SMAP and NLDAS
512 are used for soil moisture blending with TC error estimation (Fig. 4d). The error ranking of the



513 three datasets from TC are K-API>API>NLDAS (Fig. 4d), and the differences among the three
514 datasets are statistically significant.

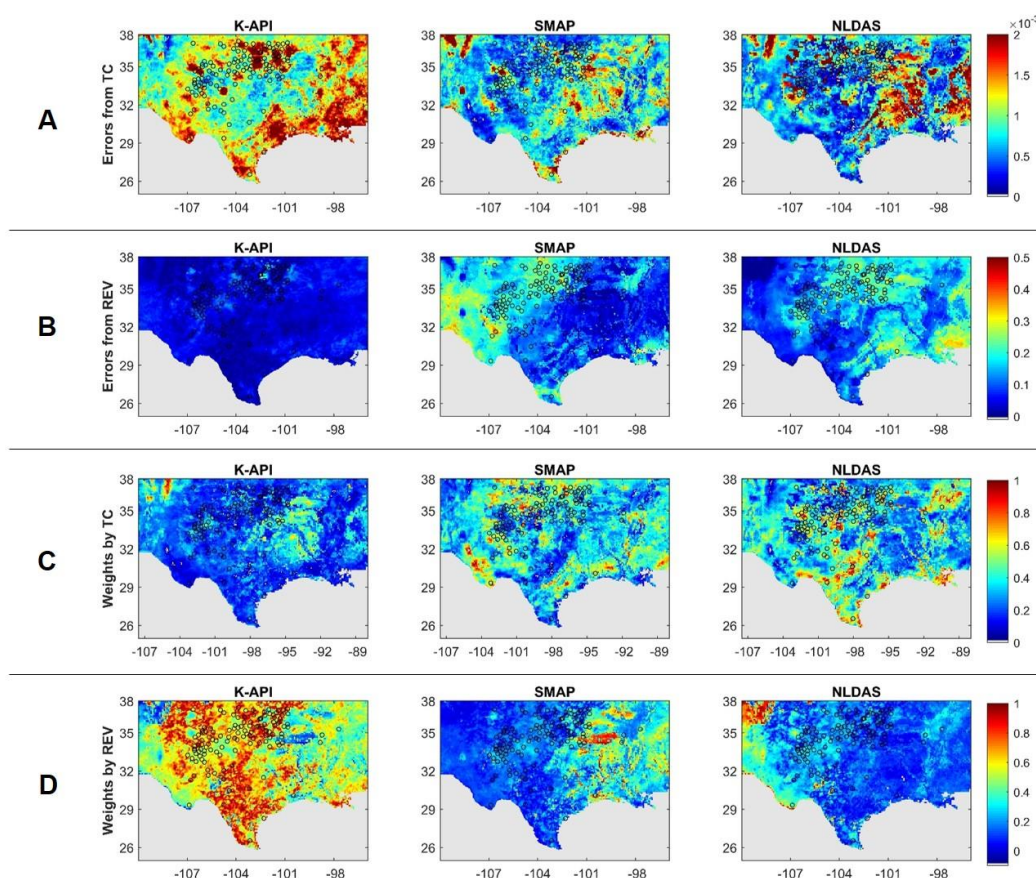
515 Our study also demonstrates that the measurement units (Fig. S4) do not impact the relative
516 relationship (error ranking) between the different datasets. It is also interesting to note that the in-
517 situ data always have relatively larger error when compared with other datasets using TC (Fig. 4a
518 to 8c). This may due to its high spatial representativeness errors (Miralles et al., 2010; Crow et al.,
519 2012b; Yilmaz et al., 2012). If this is true, then using in-situ data as the ground truth for validation
520 may not be the best choice.

521 The REV (Fig. 4e) and RK (Fig. 4f) can also be used to estimate error in different datasets.
522 REV (Fig. 4e) and RK (Fig. 4f) provide consistent results and both indicate that K-API has
523 significantly smaller errors than SMAP and NLDAS, while SMAP and NLDAS are similar (i.e.,
524 there is not a statistically significant difference between the two). Although REV is a relative ratio
525 between measurement error variance to real soil moisture variance, unlike TC, it does not depend
526 on another dataset during calculation. Therefore, REV provides a consistent estimate for each
527 product that does not change depending on the other datasets that are included. By comparing Fig.
528 4(b)-(c) with Fig. 4(e), in-situ data have larger errors than K-API based on both the TC and REV
529 methods.

530 Fig. 5A and 5B illustrate the spatial distribution of errors estimated using TC (Fig. 5A) and
531 REV (Fig. 5B) for the three parent datasets (K-API, SMAP and NLDAS). When using TC
532 estimates, the results agree well with Fig. 4d. NLDAS has the smallest error among the three, with
533 low errors found in the central and southwestern portions of the study area. The K-API has larger
534 errors near the Gulf of Mexico and in Oklahoma, while SMAP has larger errors scattered
535 throughout the study region. On the contrary, when using REV, the K-API has the smallest errors



536 among the three datasets over the entire study area, while SMAP data has larger errors in the
537 western part of the study region and NLDAS has larger errors in the eastern part of the study region.



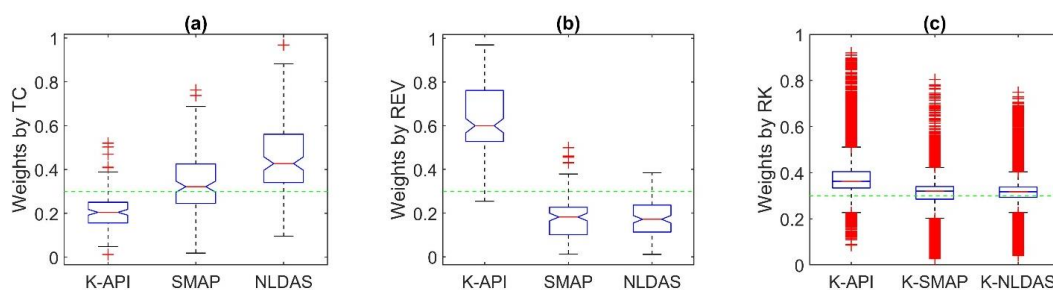
538
539 **Fig. 5** Spatial maps of errors (A and B) and LSW weights (C and D) based on errors from TC and
540 REV for each parent product. All products are in the format of absolute soil moisture. The black
541 circles indicate the locations of 127 out-of-sample stations.

542 **4.3 Weights of parent datasets**

543 Fig. 5C and 5D reveal the spatial distribution of LSW weights calculated using the errors
544 estimated from TC and REV. Fig. 6 compares the weights derived from TC, REV and RK based
545 on 127 out-of-sample stations. Generally, larger weights are given to the product with smaller



546 errors (Fig. 5), and the weighting of each product are not impacted by the data format used (Fig.
547 S5). When using TC, larger weights are given to the NLDAS (median value of 0.42) and SMAP
548 (median value of 0.32), while K-API tends to be given lower weight, with a median value about
549 0.2 (Fig. 6a). In contrast, higher weights are given to K-API (median value of 0.6), especially in
550 the central part of study area, when REV is used, while smaller weights are given to SMAP and
551 NLDAS with a median value of 0.2 for both (Fig. 6b). SMAP has higher weights in the eastern
552 part of the study region than in the west. NLDAS is given higher weights in the western part of the
553 study region (Fig. 5D). In general, the weighting scheme derived from TC (Fig. 5C and Fig. 6a)
554 has patterns that are opposite to those based on REV (Fig. 5D and Fig. 6b). It is also interesting to
555 note that the weighting scheme derived from RK (Fig. 6c) is similar to the mean weighting (0.33
556 weighting line in green). This analysis has demonstrated that the choice of weighting scheme can
557 have a substantial influence on the relative weights that are assigned to each product.

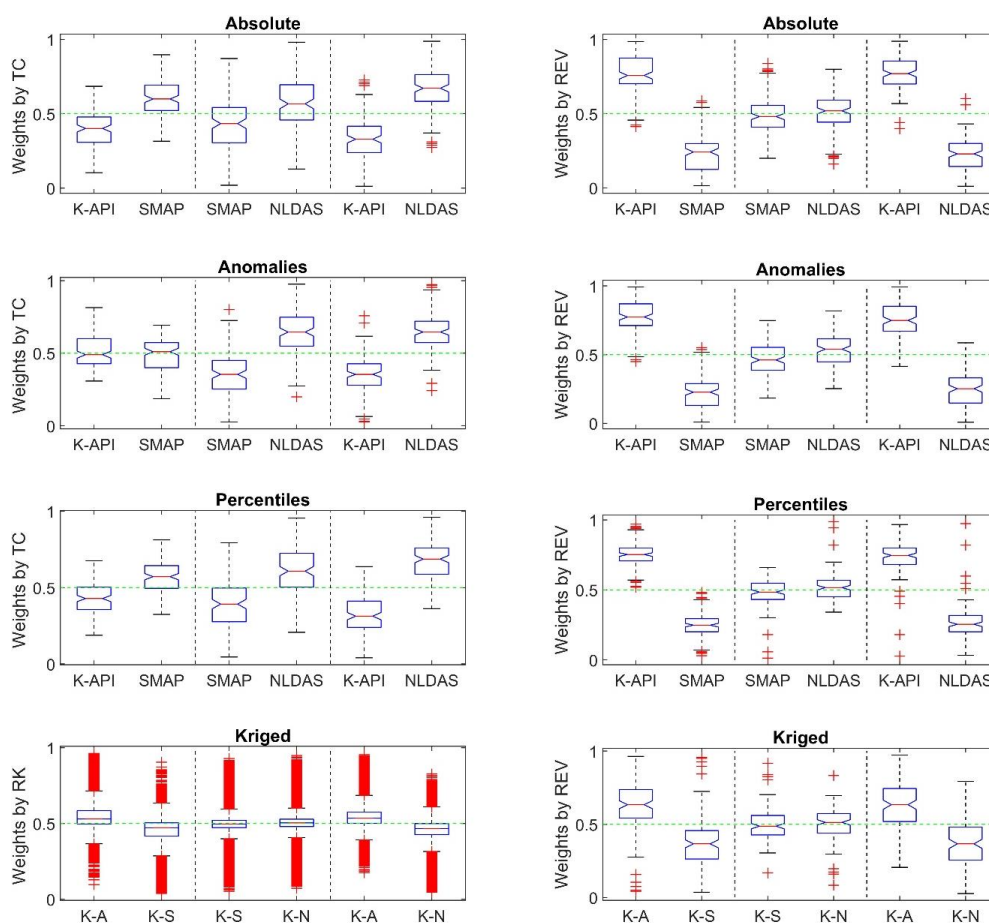


558
559 **Fig. 6** Weights of each product (K-API, SMAP and NLDAS) based on LSW using errors estimated
560 from (a) TC, (b) REV and (c) RK. The weights are calculated based on absolute soil moisture over
561 127 out-of-sample stations. The green lines indicate the averaging weighting, where each product
562 is given the same weight of 0.33.

563 Considering each dataset has errors and the inclusion of additional datasets may increase
564 the uncertainty, therefore it is important to evaluate whether it is necessary to use all three soil
565 moisture datasets to achieve the highest accuracy. Therefore, we iteratively selected pairs of the



566 parent datasets and generated a hybrid soil moisture product. The results for each combination are
 567 provided in Fig. 7. Similar to the results from Fig. 6 and Fig. S5, the TC and REV provide opposite
 568 weighting results, and the weighting from RK is similar to the simple average (equal weight of
 569 two datasets). This analysis also demonstrates that the data format has little impact on the results,
 570 especially for REV (right column in Fig. 7).



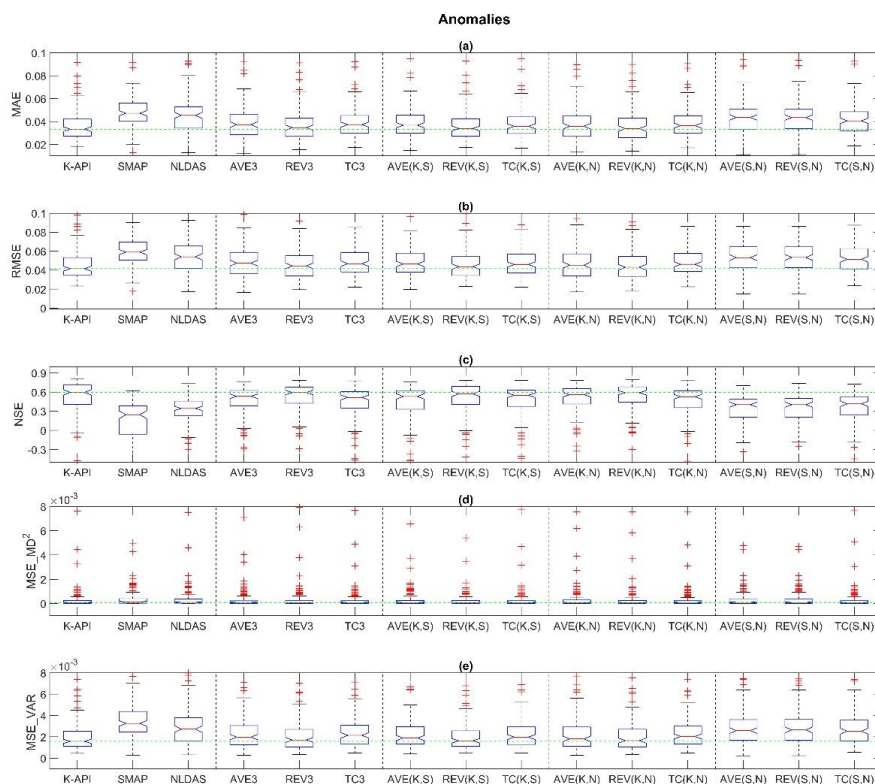
571
 572 **Fig. 7** Weights of soil moisture products in the format of anomalies (top row) and percentiles
 573 (bottom row) based on least square weighting using errors estimated from TC (left column) and
 574 REV (right column). The green line indicates the simple average weighting scheme with equal



575 weight (0.5 here) for each product. K-A is short for regression kriging using API, K-S is short for
576 regression kriging using SMAP, and K-N is short for regression kriging using NLDAS data.

577 **4.4 Evaluation of hybrid results**

578 Fig. 8 evaluates the hybrid results of soil moisture anomalies from different methods
579 (simple average (AVE), REV and TC) based on MAE, RMSE, MSE_{MD}², MSE_{VAR} and NSE.
580 The assessment of hybrid datasets in other formats (absolute values, percentiles and RK-gridded
581 soil moisture) are presented in Fig. S6, S7 and S8, respectively. In terms of MAE (Fig. 8a), K-API
582 has the smallest errors (MAE_{median} = 0.037) among the three parent datasets, while SMAP has the
583 largest errors (MAE_{median} = 0.050) and NLDAS falls in the middle (MAE_{median} = 0.046). The
584 analysis demonstrates that after blending the three parent datasets, the merged datasets do not
585 outperform the parent products, especially in comparison to K-API. Although the MAEs of the
586 AVE3, REV3 and TC3 are significantly smaller than that of SMAP and NLDAS (boxes' notches
587 do not overlap in Fig. 8a), they are not statistically significantly different from K-API (overlapped
588 notches in Fig. 8a). Our findings contrast with those of Yilmaz et al. (2012), who found that a
589 merged soil moisture product generated from ALEXI, Noah and LPRM using TC is more accurate
590 than the individual parent products. However, our study evaluated different parent datasets, and
591 the TC-based weights did vary with the input datasets (Fig. 4a-d). Since the K-API was found the
592 most accurate among the three parent products, and Yilmaz et al. (2012) did not use this product,
593 our results are not directly comparable. But both our study and Yilmaz et al. (2012) utilized
594 NLDAS Noah, and both studies found that the hybrid datasets that use NLDAS have smaller errors
595 (MAEs and RMSEs).



596

597 **Fig. 8** Comparison of parent and hybrid products of soil moisture anomalies using different
598 blending methods (simple average (AVE), REV- and TC-based) on (a) MAE, (b) RMSE, (c) NSE,
599 (d) MSE_{MD}² and (e) MSE_{VAR}. The green line indicates the median error of K-API among 127
600 out-of-sample stations. AVE3, REV3 and TC3 respectively indicate the hybrid results using all
601 three parent products based on simple average, REV and TC analysis.

602

The lack of significant improvement of the merged datasets versus the parent products may
603 be attributed to (1) sub-optimal weights because neither TC and REV consider temporal variations
604 in errors. Both TC and REV give only one error estimation at each location for the entire period.
605 In reality, the error in each parent product likely varies both spatially (from location to location)
606 and temporally (from day to day). Thus, the temporally fixed error estimation that is provided by
607 TC and REV is likely not optimal. (2) The in-situ measurements cannot be considered the “truth”



608 because they are point measurements that may not reflect the soil moisture value for each 4 km
609 grid cell. In addition, the use of in situ measurements as truth may also be biased towards the K-
610 API. As we found in Fig. 4, the in-situ soil moisture have large spatial representativeness errors.
611 Even for the densest in-situ network used in this study, such as the Oklahoma Mesonet, there is
612 only one station within each 4-km grid cell. Considering K-API is generated using in-situ soil
613 moisture, the error patterns of K-API may follow closely with that of in-situ data, which is also
614 confirmed by Fig. 4. This bias may result in smaller errors of K-API when evaluated using in-situ
615 data. (3) The validation data are not spatially exhaustive. Although 60% (127) of total stations
616 have been used in the validation, they are still relatively sparse and not evenly distributed in the
617 study area. Fig. 1 shows most validation stations are clustered in Oklahoma and west Texas, while
618 few stations are located in south Texas, Arkansas and Louisianan. It is possible that the places
619 where hybrid results showed an improvement over the parent product (K-API) are not well
620 captured using only 127 stations.

621 When comparing the results from the various blending methods, there is no statistically
622 significant difference between the merged datasets using AVE, REV or TC, even though the REV-
623 weighted datasets perform slightly better (slightly lower MAE/ RMSE, and slightly higher NSE)
624 than other two methods. This indicates that the more complicated blending methods (LSW using
625 TC and REV estimates) are not necessarily superior to the simple average. This result agrees with
626 the findings from Yilmaz et al. (2012) that the merged soil moisture anomalies using LSW and TC
627 estimates did not outperform the equally-weighted results.

628 Considering the different blending methods correspond to different weighting schemes
629 (Fig. 7 and Fig. S5), this result suggests two possible conclusions: (1) if the optimal weighting
630 (either TC- or REV-based) has been achieved, then the weighting scheme does not have a



631 significant impact on the merged results; (2) if the optimal weight has not been achieved, then
632 there is still an optimal weighting scheme to be identified that can significantly reduce the errors.
633 The evaluation of hybrid datasets using the two parent datasets (Fig. 8) suggests the first conclusion
634 (weighting scheme does not have a significant impact on the merged results) is most likely.
635 According to Fig. 6, the weights calculated using AVE, REV and TC-based methods have covered
636 all the possible weighting schemes of two datasets, including equal weighting (AVE) and two
637 cases of unbalanced weighing (the product given larger weights by TC will be given smaller
638 weights by REV). Still, no significant differences are observed when different weighting schemes
639 are applied. In this case, the simple average (equal weighting) is recommended for soil moisture
640 blending, as the more complicated weighting schemes do not outperform this approach.

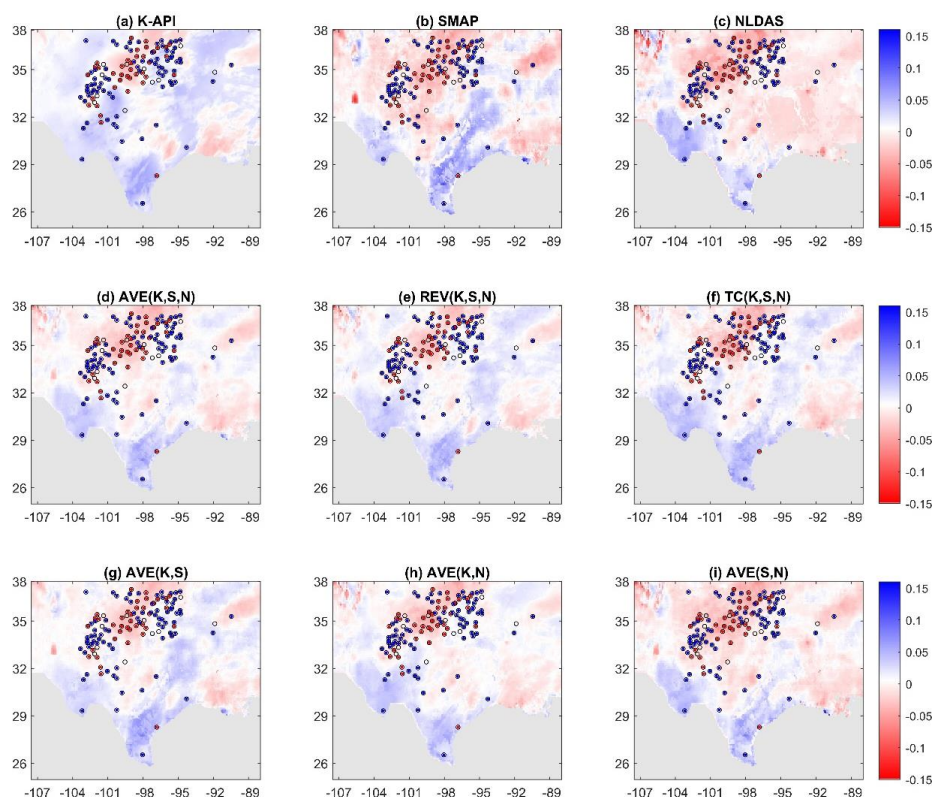
641 It is also found that the combination of SMAP and NLDAS (e.g., AVE(S,N), REV(S,N)
642 and TC(S,N)) result in a statistically significant increase in MAE values, while combining K-API
643 with either SMAP or NLDAS has similar accuracy as the merged datasets using all three datasets.
644 This indicates (1) incorporating three datasets may not be necessary to generate the most accurate
645 soil moisture product and, (2) in-situ measurement is valuable for improving the accuracy of
646 blended soil moisture datasets. K-API is the only dataset that incorporates the in-situ
647 measurements, and it has the lowest error among all parent datasets (Fig. 8). These results are
648 consistent when RMSE (Fig. 8b) or NSE (Fig. 8c) as considered instead of MAE.

649 The impact of data format on hybrid results is examined by comparing Fig. 8 with Fig. S6
650 to S8. It is found the MAE of hybrid datasets using anomalies (about $0.035 \text{ m}^3\text{m}^{-3}$) is lower than
651 that of the absolute datasets (about $0.055 \text{ m}^3\text{m}^{-3}$). The hybrid datasets using anomalies and
652 percentiles also have higher NSE (around 0.6) values than that of (around 0.3) absolute and RK-
653 gridded datasets. The improved performance of the anomaly and percentile datasets are mainly



654 due to the removal of bias error (MSE_{MD^2}). Using Eq.S2 to Eq. S4 from the Supplementary Text,
655 the MSE can be decomposed to differences in the mean or bias (MSE_{MD^2}) and differences in the
656 variance (MSE_{VAR}). It is found that the bias for both the soil moisture anomalies (Fig. 8d) and
657 soil moisture percentiles (Fig. S6d) are close to zero. Therefore, most of their error is due to
658 differences in variance (Fig. 8e and Fig. S6e). This is reasonable since both anomalies and
659 percentiles are methods for standardizing the datasets and they are useful for removing the
660 systematic bias between different data sets (Ford et al., 2015;Zhang et al., 2017a). In contrast, the
661 errors of absolute soil moisture (Fig. S7d and S7e) and RK-gridded absolute soil moisture (Fig.
662 S8d and S8e) have similar proportions of error that are due to bias ($0.02 \text{ m}^3\text{m}^{-3}$) and variance (0.02
663 m^3m^{-3}). This indicates when using soil moisture data in absolute formats, the bias-related errors
664 are present in the final datasets.

665 Fig. 9 shows maps of soil moisture anomalies on March 31, 2015 for each of the parent
666 datasets (a-c) and the merged datasets based on using three products (d-f) and two products (g-i).
667 There are distinct differences between the three parent datasets. The K-API (Fig. 9a) has a
668 smoother pattern than the other two datasets. In addition, the in-situ anomalies (with blue dots
669 indicate positive anomalies and red dots indicate negative anomalies) seem to match better with
670 that of K-API. However, the differences between the maps become less distinguishable after
671 blending the three datasets using AVE (Fig. 9d), REV- (Fig. 9e) and TC-based LSW (Fig. 9f).
672 There is also no dramatic change of spatial patterns when changing the number of input datasets
673 from three (Fig. 9d) to two (Fig. 9g-i) using simple average, which agrees with the results from
674 Fig. 8.

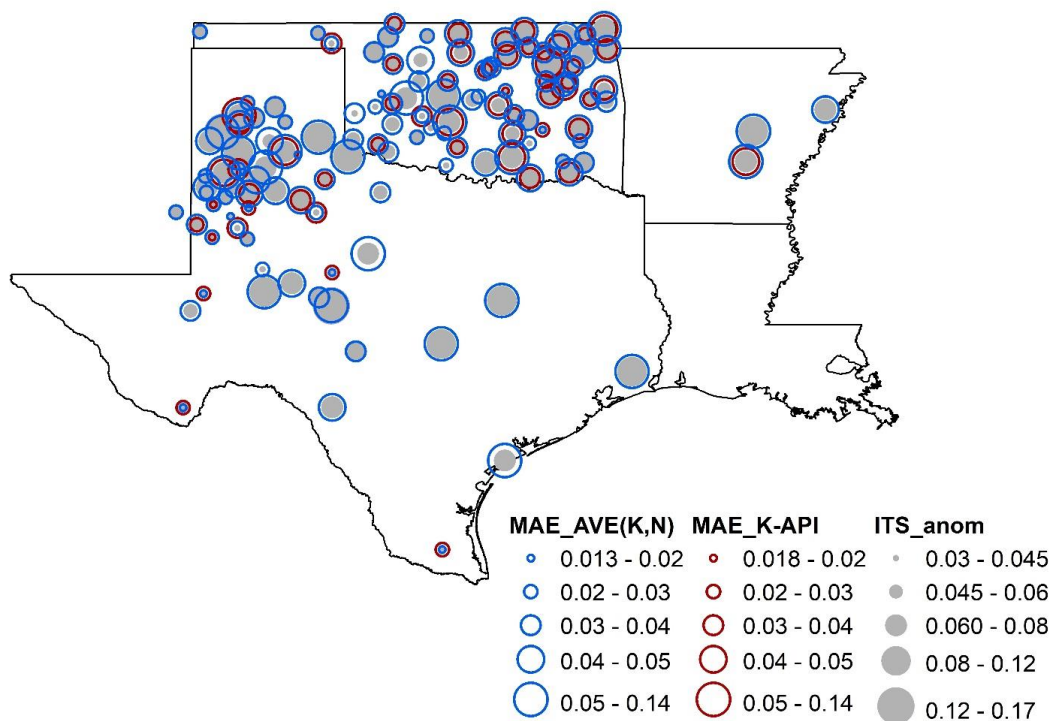


675
676 **Fig. 9** Maps of parent and hybrid products of soil moisture anomalies on March 31, 2015. (a)-(c)
677 present the three parent products (K-API, SMAP and NLDAS); (d)-(f) respectively represent the
678 hybrid product from 3 parent products using simple average, least square weighting using REV
679 estimated errors and TC estimated errors; (g)-(i) represent the hybrid products using simple
680 average of two parent products. The red dots represent the in-situ stations with negative anomalies,
681 the blue dots present the in-situ stations with positive anomalies, and the empty circles present the
682 in-situ stations with no measurement on that day.

683 Finally, the spatial patterns of errors for K-API and AVE(K,N) are shown in Fig. 10. By
684 overlaying the ITS, a consistent pattern is observed between the spatial distribution of MAE and
685 ITS (Fig. 10). That is, sites that are less temporally representative sites have higher MAE values
686 than those that are more temporally representative. This agrees with previous finding that the



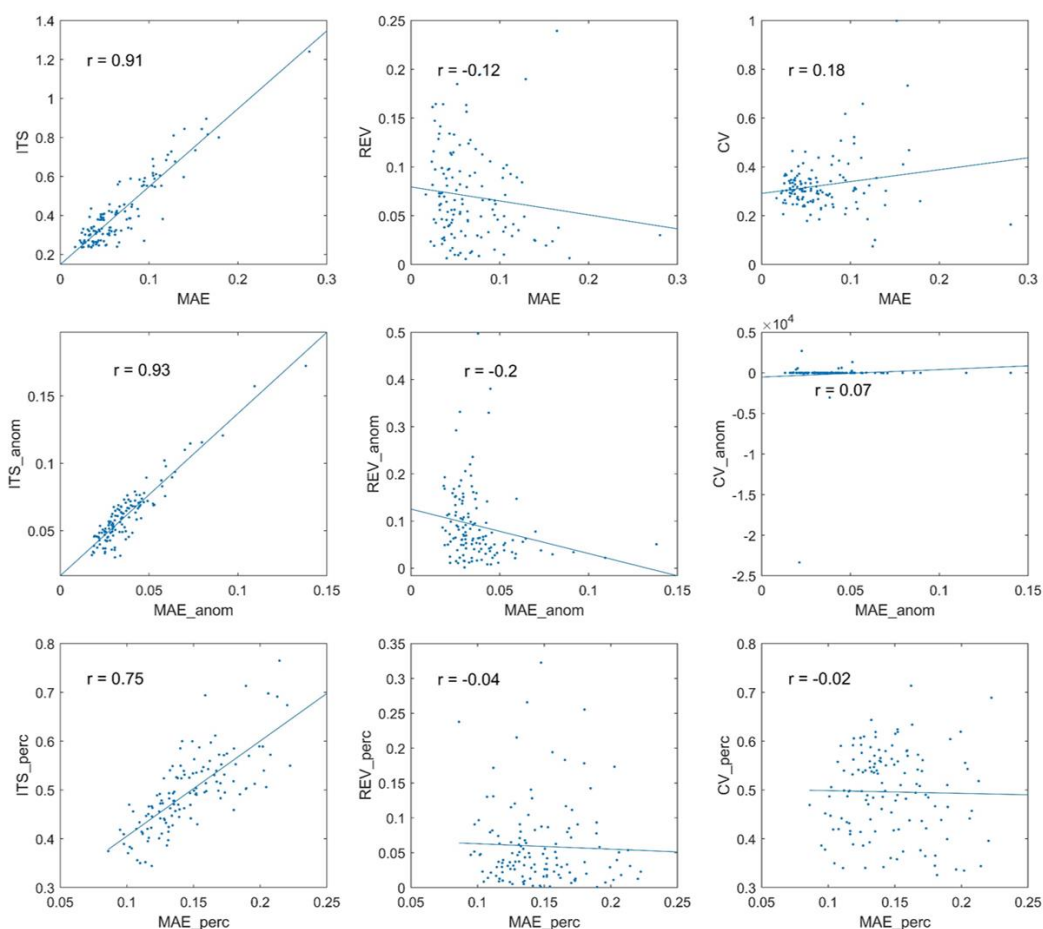
687 kriging performance declines as the data variation increases (Schläpfer and Schmid,
688 1999;Martínez-Cob, 1996;Li and Heap, 2011;Keskin and Grunwald, 2018). Gotway et al. (1996)
689 found that the performance of both inverse distance weighting and ordinary kriging declines as
690 CV increases when mapping soil properties. Based on a review of more than 50 spatial
691 interpolation studies, Li and Heap (2011) found that data variation has a significant impact on the
692 performance of spatial interpolation methods. Generally, accuracy decreases as CV increases.
693 Keskin and Grunwald (2018) also found an inverse relationship between the accuracy of RK
694 models and the variation of soil properties based on a review of more than 70 studies of RK model.



695
696 **Fig. 10** The spatial distribution of MAE of AVE(K,N), K-API and ITS index using anomalies soil
697 moisture.



698 The correlation between temporal stability and error is further demonstrated in Fig. 11. The
699 results show that the MAE has a higher correlation with ITS than REV or CV. This finding is
700 consistent for all data formats (absolute, anomalies and percentiles). As the variability in the data
701 increases, the predictive accuracy of RK decreases.

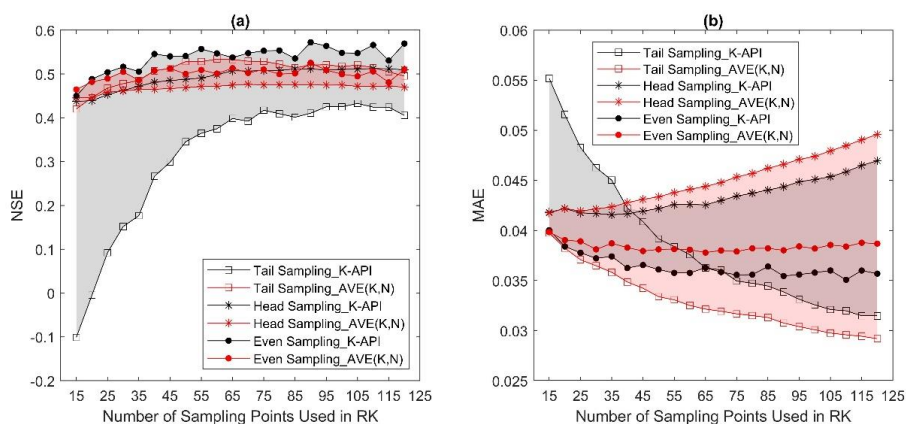


702
703 **Fig. 11** Relationship between MAE and three indices (ITS, REV and CV) using absolute soil
704 moisture (first row), anomalies (second row) and percentiles (third row).

705 Another interesting finding from Fig. 10 is that the MAEs of K-API (red circles) are
706 generally smaller than that of AVE(K,N) (blue circles), especially in Oklahoma and northwest
707 Texas. However, in places where in-situ measurements are sparse, such as the central to the south



708 of Texas and east Arkansas, the AVE(K,N) has similar and sometimes smaller MAE than K-API.
709 This indicates when in-situ measurements are sparse, using additional sources of soil moisture
710 information (such that from NLDAS) may help to increase the accuracy. To further confirm this
711 point, the assessment of K-API and AVE(K,N) with varying numbers of sampling points and
712 different sampling schemes are provided in Fig. 12 using (a) NSE and (b) MAE, respectively.
713 Three different sampling schemes are compared, including tail sampling (choosing sampling
714 points from the tail of ascending ITS), head sampling (choosing sampling points from the head of
715 ascending ITS) and even sampling (choosing sampling points evenly from the ascending ITS).
716 Since ITS is an indicator of the temporal stability, a more “representative” site is characterized
717 by a lower ITS. Therefore, the tail sampling scheme selects the least “representative” sites for RK,
718 head sampling selects the most “representative” sites for RK, while even sampling selects the sites
719 most close to the population distribution for RK.



720
721 **Fig. 12** Assessment of K-API and AVE(K,N) under different sampling scheme and sampling
722 points in terms of (a) NSE and (b) MAE. Both the NSE and MAE are calculated using the out-of-
723 sample stations over the entire study period. “Tail Sampling” indicate choosing sampling points
724 from the tail of ascending ITS (denoted by line with square), “Head Sampling” indicates choosing
725 sampling points from the head of ascending ITS (denoted by line with asterisk), while “Even



726 Sampling” indicates choosing sampling points evenly from the ascending ITS (denoted by line
727 with dot).

728 A positive NSE trend is observed as sample density increases (Fig. 12a). The most
729 significant improvement is observed for K-API using tail sampling (black line with squares). When
730 used alone, the K-API under tail sampling shows the lowest NSE values among all datasets using
731 all sampling schemes. However, when combined with the NLDAS, or the AVE(K,N) product (red
732 line with squares) using tail sampling shows comparable NSE values with other product and other
733 sampling schemes. Generally, the NSE variation of AVE(K,N) (red shaded area) under different
734 sampling schemes is much smaller than that of K-API product (grey shaded area). This indicates
735 that the hybrid product AVE(K,N) can reduce uncertainties and it is especially helpful for reducing
736 the errors caused by using too few stations or using unrepresentative stations, as compared with
737 the K-API product.

738 A decreasing trend in MAE is observed as sample density increases using both the tail and
739 even sampling schemes, which is consistent with the NSE results (Fig. 12b). Although the
740 AVE(K,N) has a larger MAE than K-API when using even sampling, the differences are not
741 statistically significant ($p > 0.05$) based on ANOVA. However, when using tail sampling, the
742 AVE(K,N) shows a statistically significant ($p < 0.05$) improvement over K-API, especially at lower
743 sample densities. The MAE of K-API is $0.055 \text{ m}^3\text{m}^{-3}$ using 15 stations, but it drops to only 0.004
744 m^3m^{-3} when AVE(K,N) is used. This indicates when sampling sites are less representative and
745 sparsely distributed, adding an extra source of soil moisture information (e.g., the product of
746 AVE(K,N)) significantly improves the accuracy. This finding has practical significance for real-
747 world applications, where achieving dense and representative sampling is always challenging. The
748 Oklahoma Mesonet is a unique and uncommonly densely network, in most cases, soil moisture



749 stations are sparsely distributed. In these cases, the hybrid product, AVE(K,N), may perform better
750 than K-API.

751 It is also worth noting that the sampling scheme has a larger impact on RK results than the
752 sample density. Although increasing the station density generally improves the accuracy, the
753 improvement gradually decreases and it levels off when the number of stations is >50 (Fig. 12a
754 and b. This agrees well with previous findings (Yuan and Quiring, 2017). In contrast, the change
755 in the sampling scheme may yield a completely different trend of MAE. As shown in Fig. 12(b),
756 an increasing trend of MAE is observed for both K-API and AVE(K,N) when head sampling is
757 adopted. This increasing trend may due to the higher degree of heterogeneity in validation data of
758 head sampling. Considering the head sampling selects the most representative sites for RK
759 modeling, while the remaining sites are less representative and have larger temporal variability,
760 which may yield larger errors. Thus, the head sampling should be avoided for RK modeling, and
761 the even sampling scheme or the bootstrapping random sampling may be more reasonable. In
762 reality, the sampling sites are always a mix of more and less representative sites.

763 In summary, both increasing sample density and adding an extra source of soil moisture
764 data can improve the accuracy, especially when the station representativeness and station density
765 are low (Fig. 12). Increasing the station density helps to capture the spatial variation of the target
766 variable, while using an additional source of soil moisture tends to lead to a more substantial
767 improvement in accuracy.

768 5. Conclusions

769 This work is the first study that compared multiple methods (REV-, TC- and RK-based
770 LSW and simple average) and considered multiple data formats (absolute, anomalies and
771 percentiles) for soil moisture blending from multiple sources, including satellite (SMAP L4-SM),



772 model (NLDAS-V2 Noah), and in-situ measurement. All soil moisture datasets are generated at 4-
773 km spatial resolution and updated daily. The results indicate that the SMAP data have a large
774 negative bias (-18%) compared with in-situ measurements (Fig. 3), thus it should be used with
775 caution without standardization, especially for drought monitoring. Both the absolute and relative
776 errors from TC vary with the input datasets (Fig. 4). In contrast, REV provides an absolute
777 measurement error, but in a relative (ratio) format. Generally, the TC-estimated error variance tend
778 to show the opposite pattern as REV. That is, the soil moisture products that have a low error
779 variance based on REV, tend to have a larger error variance using TC. The RK-estimated error
780 variances are similar for different datasets (Fig. 4 and Fig. 6).

781 The hybrid results are not sensitive to the weighting scheme that is used. There were no
782 statistically significant differences between the hybrid datasets when using different weighting
783 methods (TC, REV, RK). There is also no significant advantage to using more complicated
784 weighting (LSW) over the simple average (AVE). The merged products from two datasets (with
785 one fixed as K-API) are found to have comparable accuracy with merged products using three
786 datasets. This indicates that in-situ measurements are valuable for improving the accuracy of
787 blended soil moisture datasets. In terms of different data formats (absolute, anomalies, percentiles
788 or RK-gridded soil moisture), the NSE for anomalies and percentiles (0.60) is higher than that of
789 absolute soil moisture (0.25) mainly due to reduced biases when using anomalies and percentiles
790 (Supplementary. Fig. 6-8). However, the relative errors (or error ranking) is independent of the
791 data format used. The errors from RK are highly correlated with ITS (Fig. 10 and Fig. 11). This
792 indicates that the predictive capability of RK decreases as the heterogeneity increases.

793 Both K-API and AVE(K,N) are recommended as optimal soil moisture datasets.
794 Considering the PRISM dates back to 1895 and NLDAS dates back to 1979, a long-term soil



795 moisture record can be generated by adopting the methods in this study. It is also found K-API can
796 be used alone if the station density is high (>50 stations in our case). However, when the station
797 density is low (<50 stations) and the stations are not representative, the hybrid product (AVE(K,N))
798 has significantly better performance. Increasing station density helps to capture the spatial
799 variation of the target variable, while using an extra source of soil moisture information may help
800 to reduce the overall uncertainties (Fig. 12). This has significant practical implications for real-
801 world applications because achieving a high density of stations that are spatially representative is
802 always challenging.

803 Finally, there are some limitations of this study, such as: (1) the soil moisture products used
804 in this study were extracted with time slot covering 7 am. However, a temporal mismatch between
805 different soil moisture products may still exist due to their different temporal resolutions. Future
806 work can adopt the daily average or other methods to ensure the temporal coherence of different
807 datasets. (2) this study only considered precipitation (API) in soil moisture kriging, while in future
808 studies other variables, such as soil properties, land cover and topography (DEM), may be helpful
809 for soil moisture estimation (Ochsner et al., 2019) and should be considered to improve the
810 accuracy using RK. (3) Geographically weighted regression kriging (GWRK) (Brunsdon et al.,
811 1996; Fotheringham et al., 2003) considers the spatially non-stationarity relationships between
812 dependent variable and independent variables and weights the regression points by their distance
813 to the target point. Therefore, it may be more accurate than RK (Yang et al., 2019; Kumar et al.,
814 2012), and should be explored in future studies for estimating soil moisture. (4) Further study is
815 required to test whether these conclusions are valid in other parts of the world.

816



817 **Data Availability**

818 All datasets used in this study are publicly available. The SMAP data can be accessed through
819 National Snow and Ice Data Center (<http://nsidc.org/data/smap>). The NLDAS-V2 Noah soil
820 moisture products can be accessed through NASA's Earth Observing System Data and Information
821 System (EOSDIS) (<https://disc.gsfc.nasa.gov/>). The in-situ soil moisture measurements can be
822 accessed through the National Soil Moisture Network (<http://www.nationalsoilmoisture.com/>).

823 **Author contribution**

824 NZ designed and carried out the study under supervision of SQ. NZ prepared the original
825 manuscript and all the co-authors contributed scientifically by providing editing, comments and
826 suggestions.

827 **Competing interests.** The authors declare that they have no conflict of interest.

828 **Acknowledgement**

829 This work was financially supported by the NOAA Modeling, Analysis, Predictions and
830 Projections (MAPP) “Developing National Soil Moisture Products to Improve Drought
831 Monitoring” project (Grant number: NA17OAR4310136).

832 **References**

- 833 Abbaspour, K. C., Rouholahnejad, E., Vaghefi, S., Srinivasan, R., Yang, H., and Kløve, B.: A
834 continental-scale hydrology and water quality model for Europe: Calibration and uncertainty
835 of a high-resolution large-scale SWAT model, *Journal of Hydrology*, 524, 733-752, 2015.
- 836 Albergel, C., de Rosnay, P., Gruhier, C., Muñoz-Sabater, J., Hasenauer, S., Isaksen, L., Kerr, Y.,
837 and Wagner, W.: Evaluation of remotely sensed and modelled soil moisture products using
838 global ground-based in situ observations, *Remote Sensing of Environment*, 118, 215-226,
839 <https://doi.org/10.1016/j.rse.2011.11.017>, 2012.
- 840 Anctil, F., Michel, C., Perrin, C., and Andréassian, V.: A soil moisture index as an auxiliary ANN
841 input for stream flow forecasting, *Journal of Hydrology*, 286, 155-167,
842 <https://doi.org/10.1016/j.jhydrol.2003.09.006>, 2004.



- 843 Bi, H., Ma, J., Zheng, W., and Zeng, J.: Comparison of soil moisture in GLDAS model simulations
844 and in situ observations over the Tibetan Plateau, *Journal of Geophysical Research:*
845 *Atmospheres*, 121, 2658-2678, 2016.
- 846 Brocca, L., Melone, F., Moramarco, T., Wagner, W., Naeimi, V., Bartalis, Z., and Hasenauer, S.:
847 Improving runoff prediction through the assimilation of the ASCAT soil moisture product,
848 *Hydrology and Earth System Sciences*, 14, 1881-1893, 2010.
- 849 Brocca, L., Tullo, T., Melone, F., Moramarco, T., and Morbidelli, R.: Catchment scale soil
850 moisture spatial-temporal variability, *Journal of hydrology*, 422, 63-75, 2012.
- 851 Brunsdon, C., Fotheringham, A. S., and Charlton, M. E.: Geographically weighted regression: a
852 method for exploring spatial nonstationarity, *Geographical analysis*, 28, 281-298, 1996.
- 853 Caires, S., and Sterl, A.: Validation of ocean wind and wave data using triple collocation, *Journal*
854 *of Geophysical Research: Oceans*, 108, 2003.
- 855 Chen, F., Crow, W. T., Colliander, A., Cosh, M. H., Jackson, T. J., Bindlish, R., Reichle, R. H.,
856 Chan, S. K., Bosch, D. D., and Starks, P. J.: Application of triple collocation in ground-based
857 validation of Soil Moisture Active/Passive (SMAP) level 2 data products, *IEEE Journal of*
858 *Selected Topics in Applied Earth Observations and Remote Sensing*, 10, 489-502, 2017.
- 859 Chen, Y., Yang, K., Qin, J., Zhao, L., Tang, W., and Han, M.: Evaluation of AMSR-E retrievals
860 and GLDAS simulations against observations of a soil moisture network on the central
861 Tibetan Plateau, *Journal of Geophysical Research: Atmospheres*, 118, 4466-4475,
862 10.1002/jgrd.50301, 2013.
- 863 Cho, E., and Choi, M.: Regional scale spatio-temporal variability of soil moisture and its
864 relationship with meteorological factors over the Korean peninsula, *Journal of Hydrology*,
865 516, 317-329, 2014.
- 866 Cosh, M. H., Ochsner, T. E., McKee, L., Dong, J. N., Basara, J. B., Evett, S. R., Hatch, C. E.,
867 Small, E. E., Steele-Dunne, S. C., Zreda, M., and Sayde, C.: The Soil Moisture Active Passive
868 Marena, Oklahoma, In Situ Sensor Testbed (SMAP-MOISST): Testbed Design and
869 Evaluation of In Situ Sensors, *Vadose Zone J.*, 15, 11, 10.2136/vzj2015.09.0122, 2016.
- 870 Crow, W., and Van den Berg, M.: An improved approach for estimating observation and model
871 error parameters in soil moisture data assimilation, *Water Resources Research*, 46, W12519,
872 10.1029/2010WR009402, 2010.
- 873 Crow, W., Kumar, S., and Bolten, J.: On the utility of land surface models for agricultural drought
874 monitoring, *Hydrology and Earth System Sciences*, 16, 3451-3460, 2012a.
- 875 Crow, W. T., Berg, A. A., Cosh, M. H., Loew, A., Mohanty, B. P., Panciera, R., de Rosnay, P.,
876 Ryu, D., and Walker, J. P.: Upscaling sparse ground - based soil moisture observations for
877 the validation of coarse - resolution satellite soil moisture products, *Reviews of Geophysics*,
878 50, 2012b.
- 879 Dai, A.: Increasing drought under global warming in observations and models, *Nature Climate*
880 *Change*, 3, 52, 2013.
- 881 Daly, C., Halbleib, M., Smith, J. I., Gibson, W. P., Doggett, M. K., Taylor, G. H., Curtis, J., and
882 Pasteris, P. P.: Physiographically sensitive mapping of climatological temperature and
883 precipitation across the conterminous United States, *International Journal of Climatology: a*
884 *Journal of the Royal Meteorological Society*, 28, 2031-2064, 2008.
- 885 Delworth, T. L., and Manabe, S.: The influence of potential evaporation on the variabilities of
886 simulated soil wetness and climate, *Journal of Climate*, 1, 523-547, 1988.
- 887 Dirmeyer, P. A., Wu, J., Norton, H. E., Dorigo, W. A., Quiring, S. M., Ford, T. W., Santanello Jr,
888 J. A., Bosilovich, M. G., Ek, M. B., and Koster, R. D.: Confronting weather and climate



- 889 models with observational data from soil moisture networks over the United States, *Journal*
890 *of hydrometeorology*, 17, 1049-1067, 2016.
- 891 Dobriyal, P., Qureshi, A., Badola, R., and Hussain, S. A.: A review of the methods available for
892 estimating soil moisture and its implications for water resource management, *Journal of*
893 *Hydrology*, 458, 110-117, 2012.
- 894 Dong, J., Crow, W. T., and Bindlish, R.: The Error Structure of the SMAP Single and Dual
895 Channel Soil Moisture Retrievals, *Geophysical Research Letters*, 45, 758-765, 2018.
- 896 Dorigo, W., Scipal, K., Parinussa, R. M., Liu, Y. Y., Wagner, W., De Jeu, R. A., and Naeimi, V.:
897 Error characterisation of global active and passive microwave soil moisture data sets, 2010.
- 898 Dorigo, W., Wagner, W., Hohensinn, R., Hahn, S., Paulik, C., Xaver, A., Gruber, A., Drusch, M.,
899 Mecklenburg, S., and Oevelen, P. v.: The International Soil Moisture Network: a data hosting
900 facility for global in situ soil moisture measurements, *Hydrology and Earth System Sciences*,
901 15, 1675-1698, 2011.
- 902 Dorigo, W., Xaver, A., Vreugdenhil, M., Gruber, A., Hegyiova, A., Sanchis-Dufau, A., Zamojski,
903 D., Cordes, C., Wagner, W., and Drusch, M.: Global automated quality control of in situ soil
904 moisture data from the International Soil Moisture Network, *Vadose Zone J.*, 12, 2013.
- 905 Downer, C. W., and Ogden, F. L.: Prediction of runoff and soil moistures at the watershed scale:
906 Effects of model complexity and parameter assignment, *Water Resources Research*, 39,
907 10.1029/2002wr001439, 2003.
- 908 Eldeiry, A. A., and Garcia, L. A.: Comparison of ordinary kriging, regression kriging, and
909 cokriging techniques to estimate soil salinity using LANDSAT images, *J. Irrig. Drainage Eng-*
910 *ASCE*, 136, 355-364, 2010.
- 911 Entekhabi, D., Njoku, E. G., O'Neill, P. E., Kellogg, K. H., Crow, W. T., Edelstein, W. N., Entin,
912 J. K., Goodman, S. D., Jackson, T. J., and Johnson, J.: The soil moisture active passive (SMAP)
913 mission, *Proceedings of the IEEE*, 98, 704-716, 2010.
- 914 Fang, H., Wei, S., Jiang, C., and Scipal, K.: Theoretical uncertainty analysis of global MODIS,
915 CYCLOPES, and GLOBCARBON LAI products using a triple collocation method, *Remote*
916 *Sensing of Environment*, 124, 610-621, 2012.
- 917 Ford, T. W., and Quiring, S. M.: Comparison and application of multiple methods for temporal
918 interpolation of daily soil moisture, *International Journal of Climatology*, 34, 2604-2621,
919 2014.
- 920 Ford, T. W., Rapp, A. D., and Quiring, S. M.: Does afternoon precipitation occur preferentially
921 over dry or wet soils in Oklahoma?, *Journal of Hydrometeorology*, 16, 874-888, 2015.
- 922 Ford, T. W., Wang, Q., and Quiring, S. M.: The observation record length necessary to generate
923 robust soil moisture percentiles, *Journal of Applied Meteorology and Climatology*, 55, 2131-
924 2149, 2016.
- 925 Ford, T. W., and Quiring, S. M.: Comparison of contemporary in situ, model, and satellite remote
926 sensing soil moisture with a focus on drought monitoring, *Water Resources Research*, 55,
927 1565-1582, 2019.
- 928 Fotheringham, A. S., Brunsdon, C., and Charlton, M.: Geographically weighted regression: the
929 analysis of spatially varying relationships, John Wiley & Sons, 2003.
- 930 Gotway, C. A., Ferguson, R. B., Hergert, G. W., and Peterson, T. A.: Comparison of kriging and
931 inverse-distance methods for mapping soil parameters, *Soil Sci. Soc. Am. J.*, 60, 1237-1247,
932 1996.



- 933 Gruber, A., Dorigo, W. A., Zwieback, S., Xaver, A., and Wagner, W.: Characterizing coarse-scale
934 representativeness of in situ soil moisture measurements from the International Soil Moisture
935 Network, *Vadose Zone J.*, 12, 2013.
- 936 Gruber, A., Su, C.-H., Zwieback, S., Crow, W., Dorigo, W., and Wagner, W.: Recent advances in
937 (soil moisture) triple collocation analysis, *International Journal of Applied Earth Observation*
938 and *Geoinformation*, 45, 200-211, 2016.
- 939 Heggen, R. J.: Normalized antecedent precipitation index, *Journal of hydrologic Engineering*, 6,
940 377-381, 2001.
- 941 Hengl, T., Heuvelink, G. B., and Stein, A.: A generic framework for spatial prediction of soil
942 variables based on regression-kriging, *Geoderma*, 120, 75-93, 2004.
- 943 Hengl, T., Heuvelink, G. B., and Rossiter, D. G.: About regression-kriging: from equations to case
944 studies, *Computers & geosciences*, 33, 1301-1315, 2007.
- 945 Hirschi, M., Seneviratne, S. I., Alexandrov, V., Boberg, F., Boroneant, C., Christensen, O. B.,
946 Formayer, H., Orłowsky, B., and Stepanek, P.: Observational evidence for soil-moisture
947 impact on hot extremes in southeastern Europe, *Nature Geoscience*, 4, 17, 2011.
- 948 Huang, J., van den Dool, H. M., and Georgarakos, K. P.: Analysis of model-calculated soil
949 moisture over the United States (1931–1993) and applications to long-range temperature
950 forecasts, *Journal of Climate*, 9, 1350-1362, 1996.
- 951 Imaoka, K., Kachi, M., Kasahara, M., Ito, N., Nakagawa, K., and Oki, T.: Instrument performance
952 and calibration of AMSR-E and AMSR2, *International Archives of the Photogrammetry,*
953 *Remote Sensing and Spatial Information Science*, 38, 13-18, 2010.
- 954 Jacobs, J. M., Hsu, E. C., and Choi, M.: Time stability and variability of electronically scanned
955 thinned array radiometer soil moisture during Southern Great Plains hydrology experiments,
956 *Hydrological processes*, 24, 2807-2819, 2010.
- 957 Keesstra, S., Pereira, P., Novara, A., Brevik, E. C., Azorin-Molina, C., Parras-Alcántara, L.,
958 Jordán, A., and Cerdà, A.: Effects of soil management techniques on soil water erosion in
959 apricot orchards, *Science of the Total Environment*, 551, 357-366, 2016.
- 960 Kerr, Y. H., Waldteufel, P., Wigneron, J.-P., Martinuzzi, J., Font, J., and Berger, M.: Soil moisture
961 retrieval from space: The Soil Moisture and Ocean Salinity (SMOS) mission, *IEEE*
962 *transactions on Geoscience and remote sensing*, 39, 1729-1735, 2001.
- 963 Keskin, H., and Grunwald, S.: Regression kriging as a workhorse in the digital soil mapper's
964 toolbox, *Geoderma*, 326, 22-41, <https://doi.org/10.1016/j.geoderma.2018.04.004>, 2018.
- 965 Kohler, M. A., and Linsley, R. K.: Predicting the runoff from storm rainfall, in: *Res. Paper., US*
966 *Weather Bureau, Washington, DC*, 1951.
- 967 Koster, R. D., Dirmeyer, P. A., Guo, Z., Bonan, G., Chan, E., Cox, P., Gordon, C., Kanae, S.,
968 Kowalczyk, E., and Lawrence, D.: Regions of strong coupling between soil moisture and
969 precipitation, *Science*, 305, 1138-1140, 2004.
- 970 Kottek, M., Grieser, J., Beck, C., Rudolf, B., and Rubel, F.: World map of the Köppen-Geiger
971 climate classification updated, *Meteorologische Zeitschrift*, 15, 259-263, 2006.
- 972 Kumar, S., Lal, R., and Liu, D.: A geographically weighted regression kriging approach for
973 mapping soil organic carbon stock, *Geoderma*, 189, 627-634, 2012.
- 974 Li, J., and Heap, A. D.: A review of comparative studies of spatial interpolation methods in
975 environmental sciences: Performance and impact factors, *Ecological Informatics*, 6, 228-241,
976 <https://doi.org/10.1016/j.ecoinf.2010.12.003>, 2011.
- 977 Liang, X., Wood, E. F., and Lettenmaier, D. P.: Surface soil moisture parameterization of the VIC-
978 2L model: Evaluation and modification, *Global and Planetary Change*, 13, 195-206, 1996.



- 979 Lievens, H., and Verhoest, N. E. C.: Spatial and temporal soil moisture estimation from
980 RADARSAT-2 imagery over Flevoland, The Netherlands, *Journal of Hydrology*, 456-457,
981 44-56, <https://doi.org/10.1016/j.jhydrol.2012.06.013>, 2012.
- 982 Liu, Q., Reichle, R. H., Bindlish, R., Cosh, M. H., Crow, W. T., de Jeu, R., De Lannoy, G. J.,
983 Huffman, G. J., and Jackson, T. J.: The contributions of precipitation and soil moisture
984 observations to the skill of soil moisture estimates in a land data assimilation system, *Journal*
985 *of Hydrometeorology*, 19, 2018.
- 986 Martínez-Cob, A.: Multivariate geostatistical analysis of evapotranspiration and precipitation in
987 mountainous terrain, *Journal of Hydrology*, 174, 19-35, 1996.
- 988 McColl, K. A., Vogelzang, J., Konings, A. G., Entekhabi, D., Piles, M., and Stoffelen, A.:
989 Extended triple collocation: Estimating errors and correlation coefficients with respect to an
990 unknown target, *Geophysical Research Letters*, 41, 6229-6236, 2014.
- 991 Meng, L., and Quiring, S. M.: A Comparison of Soil Moisture Models Using Soil Climate Analysis
992 Network Observations, *Journal of Hydrometeorology*, 9, 641-659, 10.1175/2008jhm916.1,
993 2008.
- 994 Miralles, D. G., Crow, W. T., and Cosh, M. H.: Estimating spatial sampling errors in coarse-scale
995 soil moisture estimates derived from point-scale observations, *Journal of Hydrometeorology*,
996 11, 1423-1429, 2010.
- 997 Mishra, U., Lal, R., Liu, D., and Van Meirvenne, M.: Predicting the spatial variation of the soil
998 organic carbon pool at a regional scale, *Soil Sci. Soc. Am. J.*, 74, 906-914, 2010.
- 999 Mitchell, K. E., Lohmann, D., Houser, P. R., Wood, E. F., Schaake, J. C., Robock, A., Cosgrove,
1000 B. A., Sheffield, J., Duan, Q., and Luo, L.: The multi - institution North American Land Data
1001 Assimilation System (NLDAS): Utilizing multiple GCIP products and partners in a
1002 continental distributed hydrological modeling system, *Journal of Geophysical Research:*
1003 *Atmospheres*, 109, 2004.
- 1004 Mittelbach, H., and Seneviratne, S. I.: A new perspective on the spatio-temporal variability of soil
1005 moisture: temporal dynamics versus time-invariant contributions, *Hydrology and Earth*
1006 *System Sciences*, 16, 2169-2179, 2012.
- 1007 Ochsner, T. E., Linde, E., Haffner, M., and Dong, J.: Mesoscale Soil Moisture Patterns Revealed
1008 Using a Sparse In Situ Network and Regression Kriging, *Water Resources Research*, 55,
1009 4785-4800, 10.1029/2018wr024535, 2019.
- 1010 Odeha, I., McBratney, A., and Chittleborough, D.: Spatial prediction of soil properties from
1011 landform attributes derived from a digital elevation model, *Geoderma*, 63, 197-214, 1994.
- 1012 Paloscia, S., Pettinato, S., Santi, E., Notarnicola, C., Pasolli, L., and Reppucci, A.: Soil moisture
1013 mapping using Sentinel-1 images: Algorithm and preliminary validation, *Remote Sensing of*
1014 *Environment*, 134, 234-248, 2013.
- 1015 Parinussa, R. M., Meesters, A. G., Liu, Y. Y., Dorigo, W., Wagner, W., and de Jeu, R. A.: Error
1016 estimates for near-real-time satellite soil moisture as derived from the land parameter retrieval
1017 model, *IEEE Geoscience and Remote Sensing Letters*, 8, 779-783, 2011.
- 1018 Penna, D., Brocca, L., Borga, M., and Dalla Fontana, G.: Soil moisture temporal stability at
1019 different depths on two alpine hillslopes during wet and dry periods, *Journal of Hydrology*,
1020 477, 55-71, 2013.
- 1021 Pittelkow, C. M., Liang, X., Linquist, B. A., Van Groenigen, K. J., Lee, J., Lundy, M. E., Van
1022 Gestel, N., Six, J., Venterea, R. T., and van Kessel, C.: Productivity limits and potentials of
1023 the principles of conservation agriculture, *Nature*, 517, 365, 2015.



- 1024 Quiring, S. M., Ford, T. W., Wang, J. K., Khong, A., Harris, E., Lindgren, T., Goldberg, D. W.,
1025 and Li, Z.: The North American Soil Moisture Database: Development and Applications,
1026 Bulletin of the American Meteorological Society, 97, 1441-1459, 10.1175/bams-d-13-
1027 00263.1, 2016.
- 1028 Reichle, R., Lannoy, G. D., Koster, R. D., Crow, W. T., Kimball, J. S., and Liu, Q.: SMAP L4
1029 Global 3-hourly 9 km EASE-Grid Surface and Root Zone Soil Moisture Geophysical Data,
1030 Version 4. SPL4SMGP, Boulder, Colorado USA. NASA National Snow and Ice Data Center
1031 Distributed Active Archive Center, <https://doi.org/10.5067/KPJNN2GI1DQR>, 2018.
- 1032 Reichle, R. H., De Lannoy, G. J. M., Liu, Q., Ardizzone, J. V., Colliander, A., Conaty, A., Crow,
1033 W., Jackson, T. J., Jones, L. A., Kimball, J. S., Koster, R. D., Mahanama, S. P., Smith, E. B.,
1034 Berg, A., Bircher, S., Bosch, D., Caldwell, T. G., Cosh, M., González-Zamora, Á., Holifield
1035 Collins, C. D., Jensen, K. H., Livingston, S., Lopez-Baeza, E., Martínez-Fernández, J.,
1036 McNairn, H., Moghaddam, M., Pacheco, A., Pellarin, T., Prueger, J., Rowlandson, T.,
1037 Seyfried, M., Starks, P., Su, Z., Thibeault, M., van der Velde, R., Walker, J., Wu, X., and
1038 Zeng, Y.: Assessment of the SMAP Level-4 Surface and Root-Zone Soil Moisture Product
1039 Using In Situ Measurements, Journal of Hydrometeorology, 18, 2621-2645, 10.1175/JHM-
1040 D-17-0063.1, 2017.
- 1041 Robock, A., Vinnikov, K. Y., Schlosser, C. A., Speranskaya, N. A., and Xue, Y.: Use of
1042 Midlatitude Soil Moisture and Meteorological Observations to Validate Soil Moisture
1043 Simulations with Biosphere and Bucket Models, Journal of Climate, 8, 15-35, 10.1175/1520-
1044 0442(1995)008<0015:uomsma>2.0.co;2, 1995.
- 1045 Rodell, M., Houser, P. R., Jambor, U., Gottschalck, J., Mitchell, K., Meng, C.-J., Arsenault, K.,
1046 Cosgrove, B., Radakovich, J., Bosilovich, M., Entin, J. K., Walker, J. P., Lohmann, D., and
1047 Toll, D.: The Global Land Data Assimilation System, Bulletin of the American
1048 Meteorological Society, 85, 381-394, 10.1175/bams-85-3-381, 2004.
- 1049 Roebeling, R., Wolters, E., Meirink, J., and Leijnse, H.: Triple collocation of summer precipitation
1050 retrievals from SEVIRI over Europe with gridded rain gauge and weather radar data, Journal
1051 of Hydrometeorology, 13, 1552-1566, 2012.
- 1052 Schläpfer, F., and Schmid, B.: Ecosystem effects of biodiversity: a classification of hypotheses
1053 and exploration of empirical results, Ecological Applications, 9, 893-912, 1999.
- 1054 Scipal, K., Holmes, T., De Jeu, R., Naeimi, V., and Wagner, W.: A possible solution for the
1055 problem of estimating the error structure of global soil moisture data sets, Geophysical
1056 Research Letters, 35, 2008.
- 1057 Seneviratne, S. I., Corti, T., Davin, E. L., Hirschi, M., Jaeger, E. B., Lehner, I., Orlowsky, B., and
1058 Teuling, A. J.: Investigating soil moisture–climate interactions in a changing climate: A
1059 review, Earth-Science Reviews, 99, 125-161, 2010.
- 1060 Spennemann, P. C., Rivera, J. A., Saulo, A. C., and Penalba, O. C.: A Comparison of GLDAS Soil
1061 Moisture Anomalies against Standardized Precipitation Index and Multisatellite Estimations
1062 over South America, Journal of Hydrometeorology, 16, 158-171, 10.1175/jhm-d-13-0190.1,
1063 2015.
- 1064 Stoffelen, A.: Toward the true near - surface wind speed: Error modeling and calibration using
1065 triple collocation, Journal of Geophysical Research: Oceans, 103, 7755-7766, 1998.
- 1066 Su, C. H., Ryu, D., Crow, W. T., and Western, A. W.: Beyond triple collocation: Applications to
1067 soil moisture monitoring, Journal of Geophysical Research: Atmospheres, 119, 6419-6439,
1068 2014.



- 1069 Takagi, K., and Lin, H. S.: Changing controls of soil moisture spatial organization in the Shale
1070 Hills Catchment, *Geoderma*, 173-174, 289-302,
1071 <https://doi.org/10.1016/j.geoderma.2011.11.003>, 2012.
- 1072 Tian, L., and Quiring, S. M.: Spatial and temporal patterns of drought in Oklahoma (1901–2014),
1073 *International Journal of Climatology*, 39, 3365-3378, 2019.
- 1074 Vachaud, G., Passerat de Silans, A., Balabanis, P., and Vauclin, M.: Temporal Stability of
1075 Spatially Measured Soil Water Probability Density Function 1, *Soil Sci. Soc. Am. J.*, 49, 822-
1076 828, 1985.
- 1077 Vinnikov, K. Y., and Yeserkepova, I.: Soil moisture: Empirical data and model results, *Journal of*
1078 *Climate*, 4, 66-79, 1991.
- 1079 Vinnikov, K. Y., Robock, A., Speranskaya, N. A., and Schlosser, C. A.: Scales of temporal and
1080 spatial variability of midlatitude soil moisture, *Journal of Geophysical Research:*
1081 *Atmospheres*, 101, 7163-7174, 1996.
- 1082 Wagner, W., Lemoine, G., Borgeaud, M., and Rott, H.: A study of vegetation cover effects on
1083 ERS scatterometer data, *IEEE Transactions on Geoscience and Remote Sensing*, 37, 938-948,
1084 1999.
- 1085 Wagner, W., Hahn, S., Kidd, R., Melzer, T., Bartalis, Z., Hasenauer, S., Figa-Saldaña, J., de
1086 Rosnay, P., Jann, A., and Schneider, S.: The ASCAT soil moisture product: A review of its
1087 specifications, validation results, and emerging applications, *Meteorologische Zeitschrift*, 22,
1088 5-33, 2013.
- 1089 Wanders, N., Karssenber, D., Roo, A. d., De Jong, S., and Bierkens, M.: The suitability of
1090 remotely sensed soil moisture for improving operational flood forecasting, *Hydrology and*
1091 *Earth System Sciences*, 18, 2343-2357, 2014.
- 1092 Wang, A., Lettenmaier, D. P., and Sheffield, J.: Soil moisture drought in China, 1950–2006,
1093 *Journal of Climate*, 24, 3257-3271, 2011.
- 1094 Wang, T., Liu, Q., Franz, T. E., Li, R., Lang, Y., and Fiebrich, C. A.: Spatial patterns of soil
1095 moisture from two regional monitoring networks in the United States, *Journal of Hydrology*,
1096 552, 578-585, 2017.
- 1097 Xia, Y., Mitchell, K., Ek, M., Sheffield, J., Cosgrove, B., Wood, E., Luo, L., Alonge, C., Wei, H.,
1098 and Meng, J.: Continental - scale water and energy flux analysis and validation for the North
1099 American Land Data Assimilation System project phase 2 (NLDAS - 2): 1. Intercomparison
1100 and application of model products, *Journal of Geophysical Research: Atmospheres*, 117, 2012.
- 1101 Xia, Y., Sheffield, J., Ek, M. B., Dong, J., Chaney, N., Wei, H., Meng, J., and Wood, E. F.:
1102 Evaluation of multi-model simulated soil moisture in NLDAS-2, *Journal of Hydrology*, 512,
1103 107-125, <http://dx.doi.org/10.1016/j.jhydrol.2014.02.027>, 2014.
- 1104 Xia, Y., Ek, M. B., Wu, Y., Ford, T., and Quiring, S. M.: Comparison of NLDAS-2 simulated and
1105 NASMD observed daily soil moisture. Part I: Comparison and analysis, *Journal of*
1106 *Hydrometeorology*, 16, 1962-1980, 2015.
- 1107 Yang, S.-H., Liu, F., Song, X.-D., Lu, Y.-Y., Li, D.-C., Zhao, Y.-G., and Zhang, G.-L.: Mapping
1108 topsoil electrical conductivity by a mixed geographically weighted regression kriging: A case
1109 study in the Heihe River Basin, northwest China, *Ecological Indicators*, 102, 252-264,
1110 <https://doi.org/10.1016/j.ecolind.2019.02.038>, 2019.
- 1111 Yao, X., Fu, B., Lü, Y., Sun, F., Wang, S., and Liu, M.: Comparison of four spatial interpolation
1112 methods for estimating soil moisture in a complex terrain catchment, *PloS one*, 8, e54660,
1113 2013.



- 1114 Yilmaz, M., Crow, W., Anderson, M., and Hain, C.: An objective methodology for merging
1115 satellite - and model - based soil moisture products, *Water Resources Research*, 48, 2012.
- 1116 Yuan, S., and Quiring, S. M.: Comparison of three methods of interpolating soil moisture in
1117 Oklahoma, *International Journal of Climatology*, 37, 987-997, 2017.
- 1118 Zeng, Y., Su, Z., van der Velde, R., Wang, L., Xu, K., Wang, X., and Wen, J.: Blending satellite
1119 observed, model simulated, and in situ measured soil moisture over Tibetan Plateau, *Remote
1120 sensing*, 8, 268, 2016.
- 1121 Zhang, N., Quiring, S., Ochsner, T., and Ford, T.: Comparison of Three Methods for Vertical
1122 Extrapolation of Soil Moisture in Oklahoma, *Vadose Zone J.*, 16, 2017a.
- 1123 Zhang, N., Zhao, C., Quiring, S. M., and Li, J.: Winter Wheat Yield Prediction Using Normalized
1124 Difference Vegetative Index and Agro-Climatic Parameters in Oklahoma, *Agronomy Journal*,
1125 109, 2700-2713, 2017b.
- 1126 Zhao, Y., Peth, S., Wang, X., Lin, H., and Horn, R.: Controls of surface soil moisture spatial
1127 patterns and their temporal stability in a semi - arid steppe, *Hydrological Processes*, 24, 2507-
1128 2519, 2010.
1129